REPLACEMENT OF THE BASIC AND ACIDIC COMPONENTS OF MAGNESIUM POTASSIUM PHOSPHATE CEMENT WITH CALCIUM SULFOALUMINATE CEMENT AND FLY ASH PHOSPHATE SALTS

A THESIS SUBMITTED TO
THE GRADUATE SCHOOL OF NATURAL AND APPLIED SCIENCES
OF
MIDDLE EAST TECHNICAL UNIVERSITY

BY

HOSSEIN MAZAHERI SHADBAD

IN PARTIAL FULFILLMENT OF THE REQUIREMENTS
FOR
THE DEGREE OF MASTER OF SCIENCE
IN
CIVIL ENGINEERING

DECEMBER 2022

Approval of the thesis:

REPLACEMENT OF THE BASIC AND ACIDIC COMPONENTS OF MAGNESIUM POTASSIUM PHOSPHATE CEMENT WITH CALCIUM SULFOALUMINATE CEMENT AND FLY ASH PHOSPHATE SALTS

submitted by **HOSSEIN MAZAHERI SHADBAD** in partial fulfillment of the requirements for the degree of **Master of Science in Civil Engineering, Middle East Technical University** by,

Prof. Dr. Halil Kalıpçılar
Dean, Graduate School of **Natural and Applied Sciences** _____

Prof. Dr. Erdem Canbay
Head of the Department, **Civil Engineering** _____

Prof. Dr. Sinan Turhan Erdoğan
Supervisor, Civil Engineering, METU _____

Assoc. Prof. Dr. Çağla Meral Akgül
Co-Supervisor, Civil Engineering, METU _____

Examining Committee Members:

Prof. Dr. Burak Uzal
Civil Engineering, Abdullah Gül University _____

Prof. Dr. Sinan Turhan Erdoğan
Civil Engineering, METU _____

Assoc. Prof. Dr. Çağla Meral Akgül
Civil Engineering, METU _____

Asst. Dr. Güzide Atasoy Özcan
Civil Engineering, METU _____

Asst. Prof. Dr. Özlem Kasap Keskin
Civil Engineering, Muğla Sıtkı Koçman University _____

Date: 02.12.2022

I hereby declare that all information in this document has been obtained and presented in accordance with academic rules and ethical conduct. I also declare that, as required by these rules and conduct, I have fully cited and referenced all material and results that are not original to this work.

Name Last name : Hossein Mazaheri Shadbad

Signature :

ABSTRACT

REPLACEMENT OF THE BASIC AND ACIDIC COMPONENTS OF MAGNESIUM POTASSIUM PHOSPHATE CEMENT WITH CALCIUM SULFOALUMINATE CEMENT AND FLY ASH PHOSPHATE SALTS

Mazaheri Shadbad, Hossein
Master of Science, Civil Engineering
Supervisor : Prof. Dr. Sinan Turhan Erdoğan
Co-Supervisor: Assoc. Prof. Dr. Çağla Meral Akgül

December 2022, 71

Magnesium phosphate cement (MPC) is an acid-base cement with applications as a construction material. This cement has properties superior to portland cement like high early strength. However, MPC has a short setting time, high heat of hydration, and poor water resistance. In addition, this cement uses dead-burned magnesium oxide, prepared at around 1500 ˚C, which consumes much energy, releases CO_2, and increases cost. In this study, the two main components of magnesium potassium phosphate cement, dead-burned MgO and potassium dihydrogen phosphate (KH_2PO_4) are replaced with less-expensive and environmentally-friendly materials; a calcium sulphoaluminate cement and a mixture of phosphoric acid and fly ash, in three groups of mixtures. In Group I, KH_2PO_4 is replaced with the fly ash phosphate, and it is observed that the setting time is shortened, but water resistance increases significantly. In Group II, MgO is replaced with calcium sulfoaluminate cement, setting time increases up to 7 hours, and early-age compressive strength is low, but similar to the reference mix at 28 d. In Group III, both components are replaced. This group has a longer setting time than Group I and shorter than Group II as well as

lower compressive strength. Unlike in typical MPC, Reaction products of all mixtures are predominantly amorphous.

Keywords: Magnesium Phosphate Cement, Acid-Base Cement, Fly ash, Phosphoric Acid, Potassium Dihydrogen Phosphate, Calcium Sulphoaluminate Cement

ÖZ

MAGNEZYUM POTASYUM FOSFAT ÇİMENTOSUNDAKİ BAZİK VE ASİDİK BİLEŞENLERİN KALSİYUM SÜLFOALÜMİNAT ÇİMENTOSU VE UÇUCU KÜL FOSFAT TUZLARI İLE DEĞİŞTİRİLMESİ

Mazaheri Shadbad, Hossein
Yüksek Lisans, İnşaat Mühendisliği
Tez Yöneticisi: Prof. Dr. Sinan Turhan Erdoğan
Ortak Tez Yöneticisi: Doç. Dr. Çağla Meral Akgül

Aralık 2022, 71

Magnezyum fosfat çimentosu (MFÇ), inşaat malzemesi olarak kullanımı olan bir asit baz çimentosudur. Bu çimento, yüksek erken dayanım gibi Portland çimentosuna kıyasla üstün özelliklere sahiptir. Bununla birlikte, MFÇ kısa priz süresine, yüksek hidratasyon ısısına ve düşük suya dayanıklılığa sahiptir. Ayrıca bu bağlayıcı 1500 ˚C'de elde edilen ölü yanmış magnezyum oksit kullandığı için maliyeti yüksektir, büyük miktarda enerji gerektirir ve CO_2 salar. Bu çalışmada, MFÇ çimentosunun iki ana bileşeni, ölü yanmış MgO ve potasyum dihidrojen fosfat, daha ucuz ve çevre dostu malzemeler olan kalsiyum sülfoalüminat çimentosu ve bir fosforik asit-uçucu kül karışımı ile üç grup olarak ikame edilmiştir. Grup I'de KH_2PO_4, uçucu kül fosfat ile ikame edilmiştir. Bu karışımlarda priz süresinin kısaldığı ve suya dayanıklılığın önemli ölçüde arttığı gözlenmiştir. Grup II'de MgO yerine kalsiyum sülfoalüminat çimentosu kullanılmıştır. Bu karışımlarda priz süresi 7 saate kadar çıkmış ve basınç dayanımı erken yaşlarda düşük olsa da 28. günde referans karışımınkine yaklaşmıştır. Grup III'te iki bileşen de ikame edilmiştir. Bu karışımların prizsüresi Grup I'dekilere kıyasla uzun, Grup II'dekilere kıyasla kısadır. Üç grup arasında en

düşük basınç dayanımına sahip olanlar bu gruptakilerdir. Tipik MFÇ'lerdekinin aksine, tüm karışımlarda oluşan tepkime ürünleri ağırlıklı olarak amorftur.

Anahtar Kelimeler: Magnezyum Fosfat Çimentosu, Asit-Baz Çimentosu, Uçucu Kül, Fosforik Asit, Potasyum Dihidrojen Fosfat, Kalsiyum Sülfoalüminat Çimentosu

To Mahsa Amini

ACKNOWLEDGMENTS

My sincere thanks to all the people who have contributed to this thesis during the last three years. My deepest gratitude goes first and foremost to Prof. Sinan Turhan Erdoğan, my supervisor, for his constant encouragement and support, valuable ideas, and suggestions. Without his consistent and illuminating instruction, this thesis could not have reached its present form.

I wish to express my heartful gratitude to Assoc. Prof. Çağla Meral Akgül, my co-supervisor, for her great help in the critical points during this study. I am also extremely grateful to my committee members for their time and efforts.

I am thankful for the friendship of my colleagues Sepehr Seyedian, Aykut Bilginer, Batuhan Bilmez. I learned a great deal from their critical comments and suggestions. I am also appreciative of the assistance from the technicians in the Department of Civil Engineering: Cuma Yıldırım and Gülşah Bilici.

I am grateful to Yalda Gholipour, Amirhossein Fathipour, Sana Sadreddini, Amirahmad Vakilinezhad Asle Khilijani, Ali Pourabdollah, and Gelareh Tanideh, who were like a family to me in Ankara. The precious experience of living together with you will be in my heart as the most beautiful memory.

Finally, I owe much to my family for always believing in me and encouraging me to achieve my goals. Without their encouragement and understanding, it would not have been possible for me to finish this work.

TABLE OF CONTENTS

ABSTRACT v

ÖZ vii

ACKNOWLEDGMENTS x

TABLE OF CONTENTS xi

LIST OF TABLES xv

LIST OF FIGURES xvi

1 INTRODUCTION 1

1.1 Background 1

1.2 Objectives and Scope of the Thesis 2

2 LITERATURE REVIEW 3

2.1 Phosphate Cements 3

2.1.1 Magnesium Phosphate Cement 4

2.1.1.1 Raw Materials in Magnesium Phosphate Cement 4

2.1.1.2 Reaction Products in Magnesium Phosphate Cement 5

2.1.1.3 Properties of Magnesium Phosphate Cement 9

2.1.1.3.1 Compressive Strength 9

2.1.1.3.2 Setting Time 11

2.1.1.4 Major Drawbacks of Magnesium Phosphate Cement 14

2.1.1.5 Effect of Additives and Modifications on Properties of Magnesium Phosphate Cement 15

2.1.1.5.1 Wollastonite 15

2.1.1.5.2 Usage of Fly Ash, Steel Slag, and Silica Fume in MPC 16

2.1.1.5.3 Aluminum-Containing Materials 19
2.1.1.5.4 Dolomite-Bauxite-Gypsum Clinkers 21
2.1.1.6 Applications of Magnesium Phosphate Cement 22
3 MATERIALS AND EXPERIMENTAL PROCEDURE 23
3.1 Materials 23
3.1.1 Dead-Burned Magnesia Powder 23
3.1.2 Fly Ash 24
3.1.3 Monopotassium Dihydrogen Phosphate 25
3.1.4 Phosphoric Acid 25
3.1.5 Borax 25
3.1.6 Aggregate 25
3.1.7 Calcium Sulphoaluminate Clinker 27
3.1.7.1 Clinker Production 31
3.1.8 Fly Ash Phosphate ($FAPO_4$) 33
3.1.8.1 Preparation of $FAPO_4$ 34
3.2 Experimental Procedure 35
3.2.1 Groups of Phosphate Cement Mixtures 35
3.2.2 Preparation of Mortar Samples 36
3.2.3 Mixing Process 36
3.2.4 Preparation and Compressive Strength of Preliminary Samples 36
3.2.5 Mix Design of Standard Samples 39
3.2.6 Determination of Compressive Strength 39
3.2.7 Determination of Water Resistance 40
3.2.8 Determination of Setting Time 40

3.2.9 X-Ray Diffraction Analysis 40
3.2.10 Scanning Electron Microscopy 41
3.2.11 Thermal Analysis 41
3.2.12 X-ray Fluorescence Analysis 41
4 RESULTS AND DISCUSSION 42
4.1 Compressive Strength 42
4.1.1 MgFAz Mixes (Group I) 42
4.1.2 CxKH Mixes (Group II) 43
4.1.3 CxFAz Mixes (Group III) 45
4.2 Setting Time 46
4.2.1 MgFAz and CxFAz Mixes (Groups I and III) 46
4.2.2 CxKH Mixes (Group II) 46
4.3 X-Ray Diffraction Analysis 48
4.3.1 MgFAz and CxFAz Mixes (Groups I and III) 48
4.3.2 CxKH Mixes (Group II) 49
4.4 Scanning Electron Microscopy Analysis 50
4.4.1 MgFAz Mix (Group I) 50
4.4.2 CxKH Mixes (Group II) 52
4.4.3 CxFAz Mixes (Group III) 56
4.5 Thermogravimetric Analysis 57
4.5.1 Clinkers 57
4.5.2 MgFAz and CxFAz mixes (Groups I and III) 58
4.5.3 CxKH Mixes (Group II) 58
4.6 Resistance to Water 59

4.6.1 MgFAz and CxFAz Mixes (Groups I and III) 59
4.6.2 CxKH Mixes (Group II) 60
5 CONCLUSIONS AND RECOMMENDATIONS 62
5.1 Conclusions 62
5.2 Recommendations for Future Studies 63
REFERENCES 65
APPENDICES 70
APPENDIX A 70

LIST OF TABLES

Table 3.1 Oxide composition of reactive magnesium oxide and Çatalağzı fly ash 24
Table 3.2 Cumulative passing (%) sieve analyses of sands and their mixture 26
Table 3.3. Oxide composition of raw materials for clinker 27
Table 3.4. Raw materials proportions (%) of C$\bar{S}$A 28
Table 3.5. Oxide composition of selected C$\bar{S}$A 30
Table 3.6. Mix proportions for $FAPO_4$ and comparison of their PO_4 molar ratio with KH_2PO_4 33
Table 3.7 Mixture Groups 35
Table 3.8. Preliminary mixtures of MgFAz (Group I) 37
Table 3.9. Preliminary mixtures of CxKH (Group II) 38
Table 3.10. Preliminary mixtures of CxFAz (Group III) 38
Table 3.11. Mix design used to prepare the standard samples 39
Table 4.1 Element wt % of point 1 in Figure 4.8 51
Table 4.2 Element wt % of points 2 and 3 in Figure 4.9 53
Table 4.3 Element wt % of point 4 in Figure 4.11 55
Table 4.4 Element wt % of points 5 and 6 in Figure 4.12 57

LIST OF FIGURES

Figure 2.1 MgO: a) Reactive, calcined at 600-700℃; b) Calcined at 1200 ℃; c) Calcined at 1600 ℃ (Li et al., 2014). Scale bars show 10 µm. 5
Figure 2.2 XRD results of MPC pastes prepared with KH_2PO_4 at different ages. The Mg/P molar ratio of this paste is 5. (Bilginer & Erdoğan, 2021) 6
Figure 2.3 SEM image of K-Struvite in Magnesium Phosphate Cement samples (Bilginer & Erdoğan, 2021) 7
Figure 2.4 XRD pattern of reaction products of MPC in different pHs. "+" stands for newberyite, and "*" for K-struvite (Le Rouzic et al., 2017) 8
Figure 2.5 Formation steps of K-struvite (Le Rouzic et al., 2017) 8
Figure 2.6 Effect of KH_2PO_4 to MgO molar ratio on compressive strength of MPC paste samples (Li et al., 2014) 9
Figure 2.7. Effect of W/B (L/S in this study) on the compressive strength of the MPC (A. J. Wang et al., 2013). 10
Figure 2.8. Effect of 1-5 % borax by mass MgO on the compressive strength of MPC at different ages (Yang & Qian, 2010) 11
Figure 2.9 Effect of different retarders on setting time of the MPC mortars (Hall et al., 2001) 12
Figure 2.10. Influence of M/P on the compressive strength of MPC pastes (Bilginer & Erdoğan, 2021) 13
Figure 2.11. Effect of W/B (W/C in this study) ratio on the setting time of MPC pastes (Li & Chen, 2013) 13
Figure 2.12. Temperature evolution of MPC mixes with and without alumina. Alumina content is increased from M1 to M4 (Liu & Chen, 2016). All the samples have a constant volume of 64 cm^3. 14
Figure 2.13. Effect of different amounts of wollastonite on MPC paste compressive strength (Xu et al., 2020). Curve 27-W-P025 shows the mixes with wollastonite and W/B = 0.25, 27-C-P025 shows the mix without wollastonite and W/B = 0.25,

27-W-P05 is for mix with wollastonite and W/B = 0.5. In all mixes, 20 % wollastonite is added. 15
Figure 2.14. Effect of fly ash content on the compressive strength of MPC mortars (Li & Chen, 2013). 16
Figure 2.15. The adverse effect of fly ash on the compressive strength of MPC (Bilginer & Erdoğan, 2021) 17
Figure 2.16. Effect of SS: a) on compressive strength b) on the water resistance, of MPC paste samples (Ruan et al., 2022) 18
Figure 2.17. Effect of the total content of FA and SF: a) 10 %; b) 20 %; c) 30 %; d) 40 % on compressive strength of MPC (Feng et al., 2022) 19
Figure 2.18. Effect of replacement of MgO with FAC on: a) the setting time; b) the compressive strength, of MPC (Jia et al., 2019) 20
Figure 2.19. Influence of low-grade bauxite on the compressive strength of the MPC mortar samples (Liu et al., 2020) 21
Figure 2.20. Changes in the paste compressive strength of DBG produced at different calcination temperatures (T1200: 1200 °C, T1250: 1250 °C, T1300: 1300 °C) and cured in different conditions (Yu et al., 2020) 22
Figure 3.1 Obtained standard sand gradation compared with the ranges allowed in ASTM C33 (2018). 26
Figure 3.2. Melted clinker (brownish part) on the furnace plate in the calcination process 29
Figure 3.3 XRD results for clinkers. G: Gehlenite, C: Hercynite, B: Brownmillerite, Y: Ye'elimite, L: Larnite 31
Figure 3.4. a) Powder mix of clinker raw materials, b) Paste after mixing of raw materials with water, c) Underlayer used for putting clinker paste d) Final form of clinker preparation (ball-shaped samples are used) 32
Figure 3.5. Process of clinker production 33
Figure 3.6. $FAPO_4$: a) Raw materials, b) After mixing the raw materials. 34
Figure 3.7. Process of $FAPO_4$ production 35
Figure 3.8. Mixing process for preparing mortars 36

Figure 3.9. Cubes with 2.5 cm sides: a) Mold used for preliminary tests; b) Prepared samples. 37
Figure 4.1 Compressive strength development of MgFAz (Group I) 43
Figure 4.2 Compressive strength development of CxKH (Group II) and reference mix 44
Figure 4.3 Compressive strengths development of the reference mix, C4FA1, and MgFA1 45
Figure 4.4. Penetration vs. time graph in setting time test of MgFA1, C4FA1, and the reference mix (Groups I and III, and R) 46
Figure 4.5 Penetration vs. time graph in setting time test of CxKH and the reference mix 47
Figure 4.6 XRD result of a) MgFA1 mix, b) C4 and C4FA1 mix, c) Reference mix 49
Figure 4.7 XRD pattern of C3 and C3KH 50
Figure 4.8 SEM images of MgFA1 (Group I) 51
Figure 4.9 SEM images of C1KH 53
Figure 4.10 SEM images of C3KH 54
Figure 4.11 SEM images of C4KH 55
Figure 4.12 SEM images of C4FA mix 56
Figure 4.13 Mass loss of clinkers 57
Figure 4.14 Mass loss of MgFA, C4FA, and reference mixes 58
Figure 4.15 Mass loss of CxKH mixes 59
Figure 4.16 Compressive strength retention of the reference, MgFA1 and C4FA1 mixes after immersing in water 60
Figure 4.17 Compressive strength of the reference and CxKH mixes after immersing in water 61
Figure A.5.1 XRD pattern of C1 and C1KH 70
Figure A.5.2 XRD pattern of C2 and C2KH 70
Figure A.5.3 XRD pattern of C4 and C4KH 71

CHAPTER 1

INTRODUCTION

1.1 Background

Portland cement is the most-used construction binder. This cement is obtained by calcination of raw materials like limestone and clay, around 1450 ˚C, which causes ~900 kg emission of CO_2 for 1000 kg of this cement. During the last decades, there have been studies to reduce the CO_2 emission in portland cement production and improve its properties. Some alternatives to Portland cement include calcium sulphoaluminate cement, calcium aluminate cement, and alkali-activated cement. Acid-base cements have also received attention as a construction material. Among acid-base cements, magnesium phosphate cement (MPC) is the most commonly used type in construction. The reason for this attention is the superior properties of MPC in comparison to Portland cement, like high early strength, high abrasion resistance, and good bond strength. However, MPC has disadvantages like short setting time, high heat of hydration, and low water resistance. In this cement, magnesium oxide is used as the basic component, and potassium dihydrogen phosphate (KH_2PO_4) is used as the acidic component. However, to be used in MPC, magnesium oxide needs to be calcined at 1500 ˚C, which demands a large amount of energy and causes emission of CO_2. Also, potassium dihydrogen phosphate salt is an expensive material to be used on a large scale. Therefore, researchers have been working on mitigating these problems.

1.2 Objectives and Scope of the Thesis

This research focused on the improvement of MPC and its objectives are:

- to replace the basic component of MPC with a more environment-friendly material
- to increase the setting time of the MPC
- to replace KH_2PO_4 with phosphate prepared using fly ash, as the phosphorus source
- to investigate the resistance of the new material to water

This thesis is composed of five chapters: Chapter 1 states the aim of this study. In Chapter 2, a review of the literature on MPC properties and improvement methods is presented. Chapter 3 includes raw material properties and the procedures used to produce materials to replace the acid and base components in MPC. In Chapter 4, the result of the experiments are presented and discussed. Finally, Chapter 5 summarizes all the outcomes with some recommendations for future studies.

CHAPTER 2

LITERATURE REVIEW

The cements discussed in this thesis are examples of acid-base cements. These cements have been known since the mid-19th century, and the first acid-base cement was prepared by mixing zinc oxide powder with a zinc chloride solution (Wilson & Nicholson, 2005). Acid-base cements are known for their fast-setting nature and high-early strength. The setting and hardening of these cements is based on the reaction of a metal oxide as a base and an acidic solution, which results in the formation of a salt and water. For example, phosphoric acid or oxyacids have been mixed with bases like magnesium oxide, zinc oxide, and calcium oxide to obtain an acid-base cement (Wilson & Nicholson, 2005). Among these, phosphate cements or ceramics are of greater significance as construction materials due to their relatively low cost and the ability for their setting rates to be controlled.

2.1 Phosphate Cements

A phosphate cement is an acid-base cement, the acidic component of which is phosphoric acid or a phosphate salt. As a basic component, oxides like magnesium oxide, calcium oxide (Watanabe et al., 2006), aluminum oxide (Wagh, 2016), and zinc oxide (Jabri et al., 2012) have been used, and each of them leads to different products and behavior in terms of setting time, compressive strength, etc. These cements are also known as "chemically-bonded ceramics" because they have properties similar to those of traditional ceramics and are ionically bonded, but unlike ceramics, they are formed at room conditions by mixing with water. Ceramics typically require temperatures of ~1400-1700 ℃ (Wagh, 2016).

2.1.1 Magnesium Phosphate Cement

Magnesium phosphate cement (MPC) is a type of phosphate cement in which MgO is used as the base. Between the years of 1988 and 2002, only six percent of abstracts on phosphate ceramics were related to structural materials (Wagh, 2016). Most of the research was on bone treatments and implants in dentistry. However, in the last decade, this material has attracted the attention of engineers for use in construction.

MPC has many useful properties, like high early strength. Despite these many advantageous properties, this cement still has some drawbacks hindering its use in construction, which can be reviewed from different aspects. First, this cement sets very quickly, and retarders are needed to control the setting time (Jia et al., 2019). Also, this cement has low water resistance due to the presence of struvite minerals, which dissolve at low pH (Li et al., 2016; Yang et al., 2000). From another aspect, this cement requires calcination of MgO at high temperatures, around 1500 °C, which causes consuming more energy and, subsequently, releases more CO_2 than using raw magnesium oxide.

2.1.1.1 Raw Materials in Magnesium Phosphate Cement

Typical reactants in magnesium phosphate cement are a phosphate solution and dead-burned magnesium oxide (MgO). Raw magnesium oxide cannot be used because it has high reactivity and reacts in a few seconds, however, by calcination, this reactivity decreases. The high reactivity of raw magnesium oxide is due to amorphous particles on the surfaces of particles and can be reduced by calcination to make it more crystalline and increase particle size, as can be seen in Figure 2.1 (Li et al., 2014). Pure phosphoric acid isn't applicable as an acidic component either. In this case, reactions take place in a few seconds since the dissolution of phosphoric acid in water is rapid, and the initial pH of the acidic solution is low. The solubility of MgO at this low pH is high and more phosphorus is available to react with Mg^{2+}

ions. Therefore, phosphate salts are preferred because they have lower solubility and higher initial pH than pure phosphoric acid, which facilitates proper mixing and allows the casting of samples within a longer time (Mahyar & Erdoğan, 2015). Among the various phosphate salts used, the most common ones are potassium dihydrogen phosphate (KH_2PO_4) and ammonium dihydrogen phosphate ($NH_4H_2PO_4$). However, KH_2PO_4 is preferred because ammonium dihydrogen phosphate has issues like releasing ammonia, which is dangerous for human health (Le Rouzic et al., 2017).

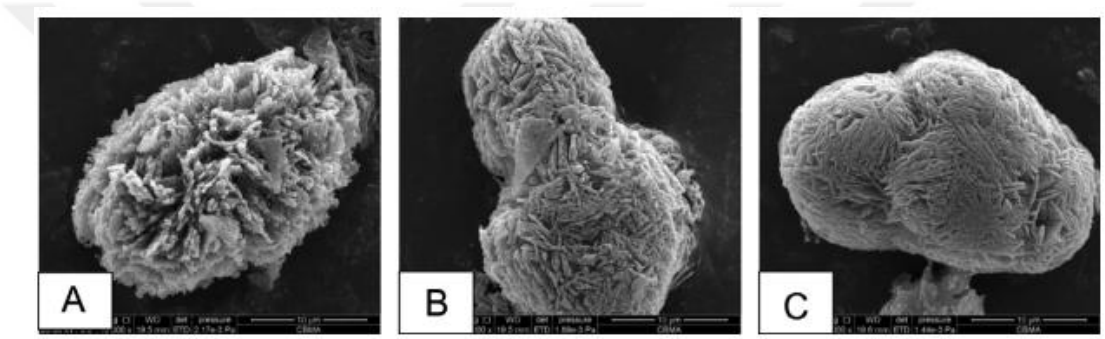


Figure 2.1 MgO: a) Reactive, calcined at 600-700℃; b) Calcined at 1200 ℃; c) Calcined at 1600 ℃ (Li et al., 2014). Scale bars show 10 µm.

2.1.1.2 Reaction Products in Magnesium Phosphate Cement

The products of the reaction between an acid and a base are salt and water. In the case of magnesium phosphate cement, using $NH_4H_2PO_4$ or KH_2PO_4, the possible reactions are:

$$MgO + NH_4H_2PO_4 + 5H_2O \rightarrow MgNH_4PO_4.6H_2O \quad (1)$$

$$MgO + KH_2PO_4 + 5H_2O \rightarrow MgKPO_4.6H_2O \quad (2)$$

$MgNH_4PO_4$ is called struvite, and $MgKPO_4.6H_2O$ is known as K-struvite (Le Rouzic et al., 2017). As Bilginer & Erdoğan (2021) observed in X-ray diffractograms for

MPC paste samples at different ages, the main product of magnesium potassium phosphate cements is K-struvite (Figure 2.2). Over time, the intensity of periclase (MgO) reduces, and the intensity of K-struvite increases slightly.

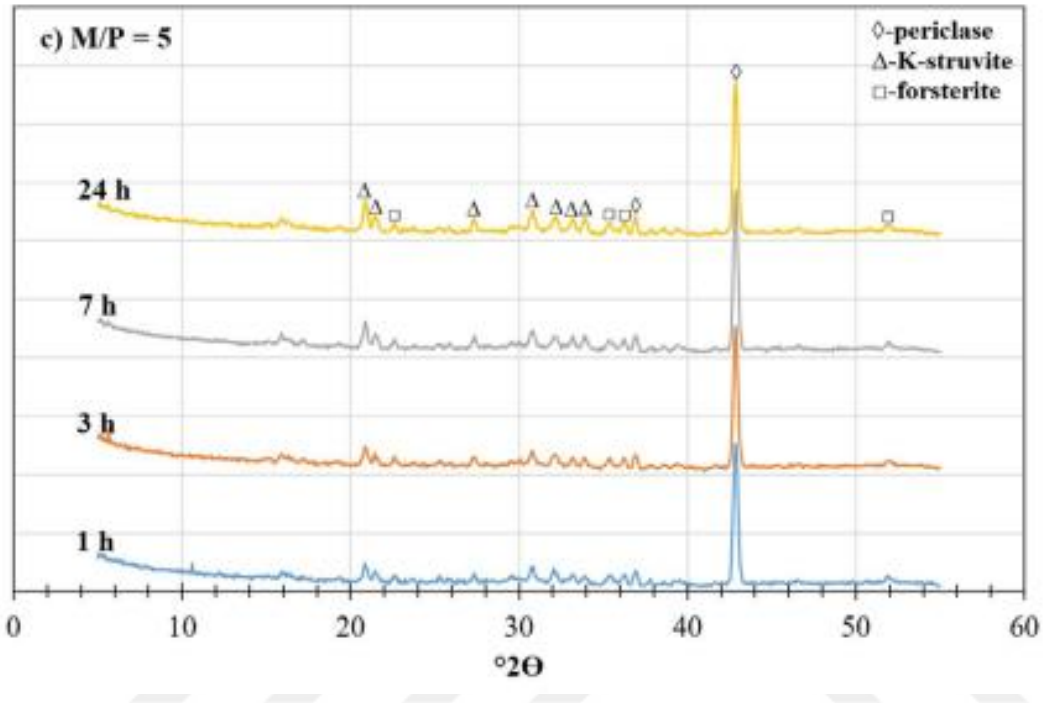


Figure 2.2 XRD results of MPC pastes prepared with KH_2PO_4 at different ages. The Mg/P molar ratio of this paste is 5. (Bilginer & Erdoğan, 2021)

In the same study, K-struvite was observed in scanning electron microscopy (SEM) images of the MPC samples (Figure 2.3). Also, some cracks are detected that can be related to the expansion of the unreacted magnesium oxide.

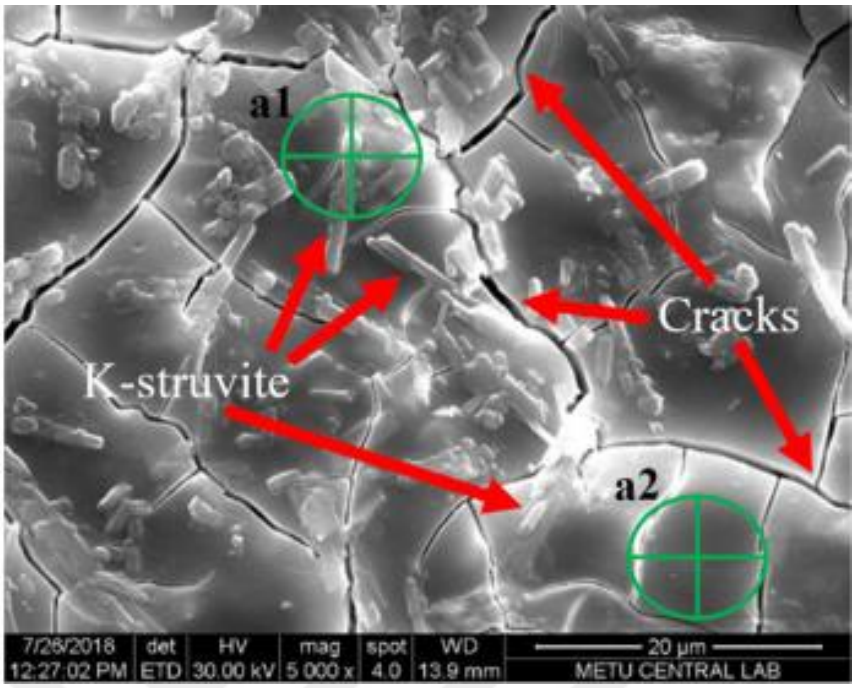


Figure 2.3 SEM image of K-Struvite in Magnesium Phosphate Cement samples (Bilginer & Erdoğan, 2021)

Different theories exist for the formation of struvite as the main reaction product of MgO and phosphate such as homogeneous nucleation, heterogeneous nucleation, and multiple precipitation/dissolution reactions (Qiao et al., 2010; Soudée & Péra, 2000; Wagh et al., 2004). However, in mixes where the phosphorous source is KH_2PO_4, there is no clear idea about how K-struvite forms. Le Rouzic et al. (2017) concluded that by the dissolution of MgO in the acidic solution (which contains K^+(aq) and $H_2PO_4^-$(aq)), newberyite ($Mg(PO_3OH).3H_2O$) forms, and then, with increasing pH, it converts to K-struvite. As shown in the XRD of this mixture (Figure 2.4) in solutions with different pH, as pH increases, more K-struvite forms, and this rise in pH occurs with the dissolution of MgO. Around a pH of 8, the dominant mineral becomes K-struvite (Figure 2.5).

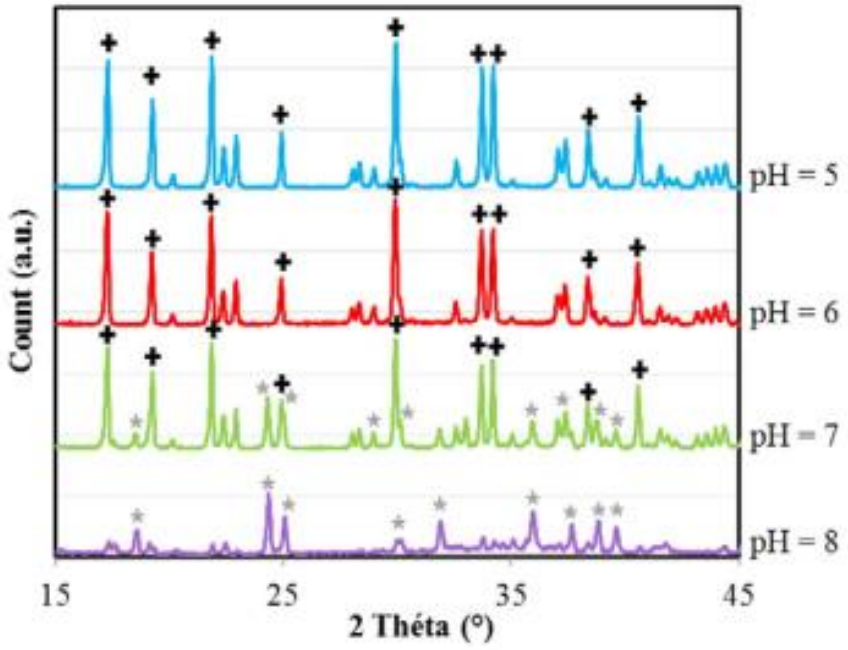


Figure 2.4 XRD pattern of reaction products of MPC in different pHs. "+" stands for newberyite, and "*" for K-struvite (Le Rouzic et al., 2017)

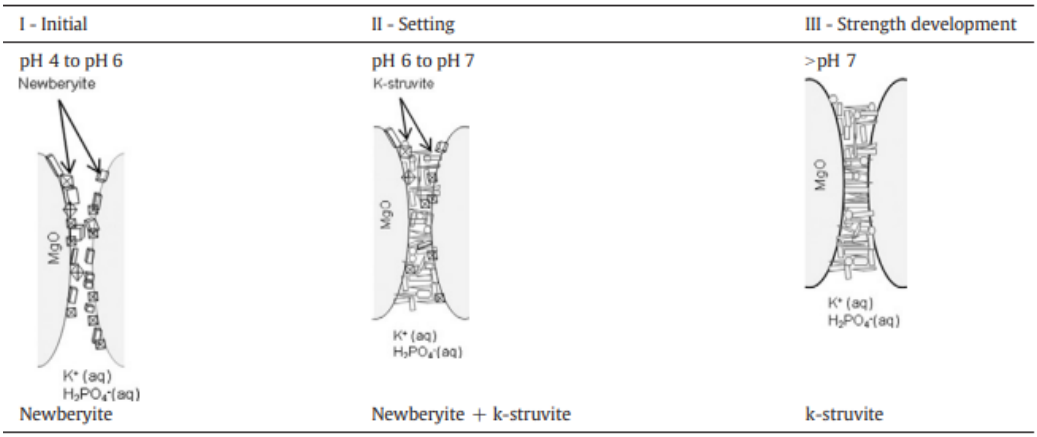


Figure 2.5 Formation steps of K-struvite (Le Rouzic et al., 2017)

2.1.1.3 Properties of Magnesium Phosphate Cement

2.1.1.3.1 Compressive Strength

MPC is known for its high early strength, however several factors can influence strength development. The main factors are the magnesium-to-phosphate molar ratio (M/P), water-to-binder ratio (W/B), retarder amount, and sand-to-binder ratio (S/B).

As M/P increases, more Mg^{2+} ions are available to participate in the reactions and form more products. Subsequently, with more final products, the compressive strength increases. However, excessive MgO content can have an adverse effect since more free MgO will remain in the sample. In Figure 2.6, it can be seen that increasing M/P up to 4 caused an increase in the compressive strength, but after that, the compressive strength decreased.

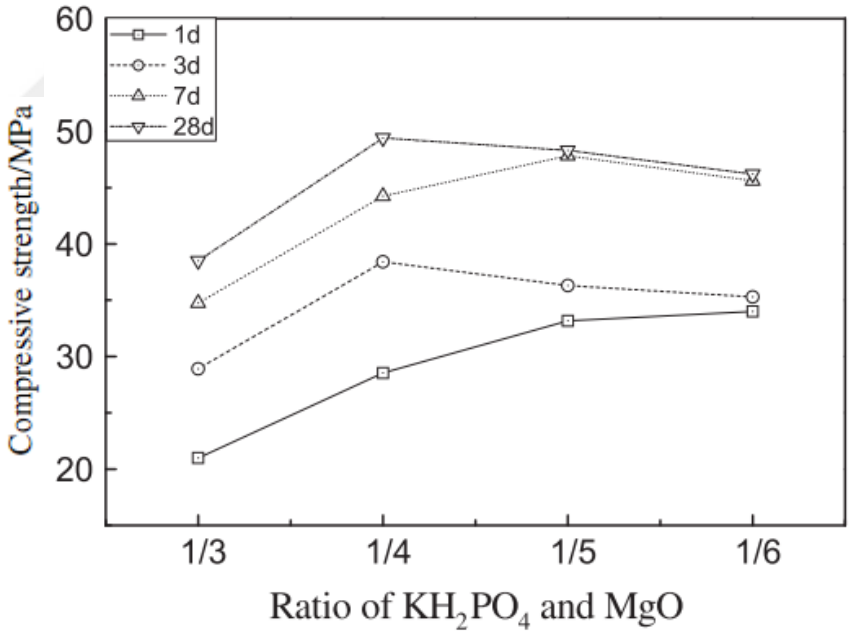


Figure 2.6 Effect of KH_2PO_4 to MgO molar ratio on compressive strength of MPC paste samples (Li et al., 2014)

In addition, with a slight change in W/B, the compressive strength changes significantly. As shown in Figure 2.7, increasing the liquid-to-solid ratio (L/S), which is the same as W/B, from 1:4 to 2:5, the compressive strength decreased from around 22 to 17 MPa. Increasing L/S caused an increase in porosity in the final paste, leading to a reduction in compressive strength.

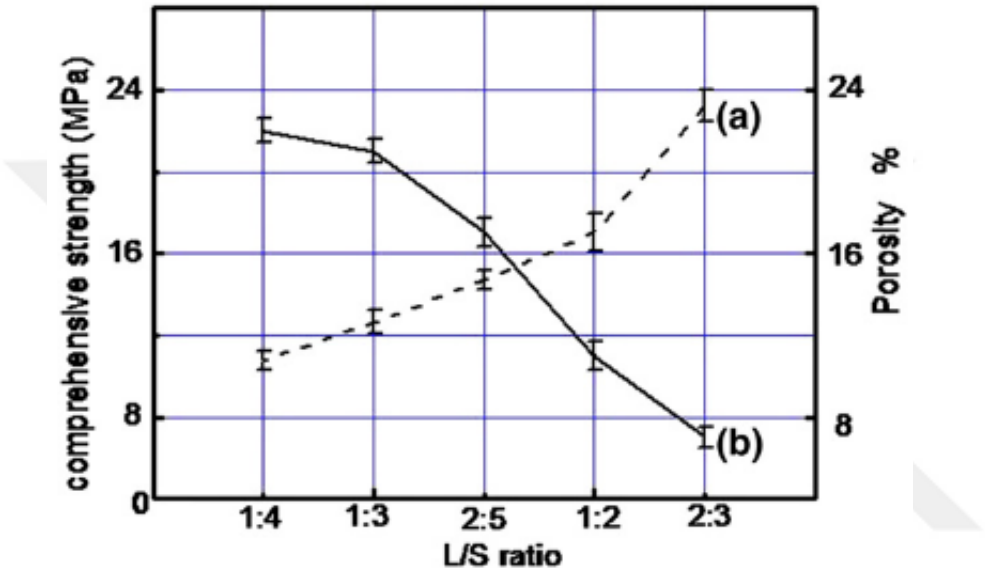


Figure 2.7. Effect of W/B (L/S in this study) on the compressive strength of the MPC (A. J. Wang et al., 2013).

Further, the setting time of MPC is less than 10 minutes generally, and retarder additives like borax to elongate the setting time are needed. However, borax negatively affects compressive strength at early ages. Yang & Qian (2010), using mixtures prepared with a constant flow, observed that increasing the borax content from 1 % to 5 % of magnesium oxide by mass decreases compressive strength at early ages (Figure 2.8).

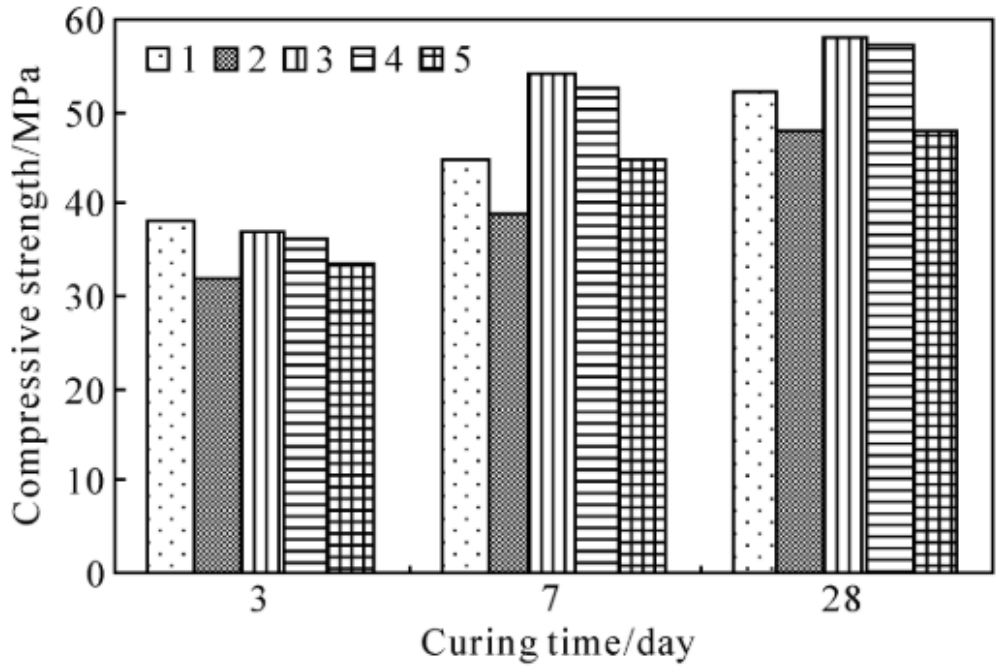


Figure 2.8. Effect of 1-5 % borax by mass MgO on the compressive strength of MPC at different ages (Yang & Qian, 2010)

Finally, S/B can also affect the compressive strength of MPC samples. It has been observed that increasing S/B reduces the paste content of the mixture and, subsequently, its compressive strength (Bilginer & Erdoğan, 2021).

2.1.1.3.2 Setting Time

Similar to compressive strength, the setting time of MPC is affected by mixture proportions. With the use of borax as a retarder, the formation of magnesium borate creates a protective film on the surface of MgO grains. This helps increase pH and decrease the initial temperature of MPC pastes, causing a retarding effect (Yang & Qian, 2010). Besides borax, boric acid can also be used as a retarder, affecting the setting time and compressive strength of MPC (Figure 2.9).

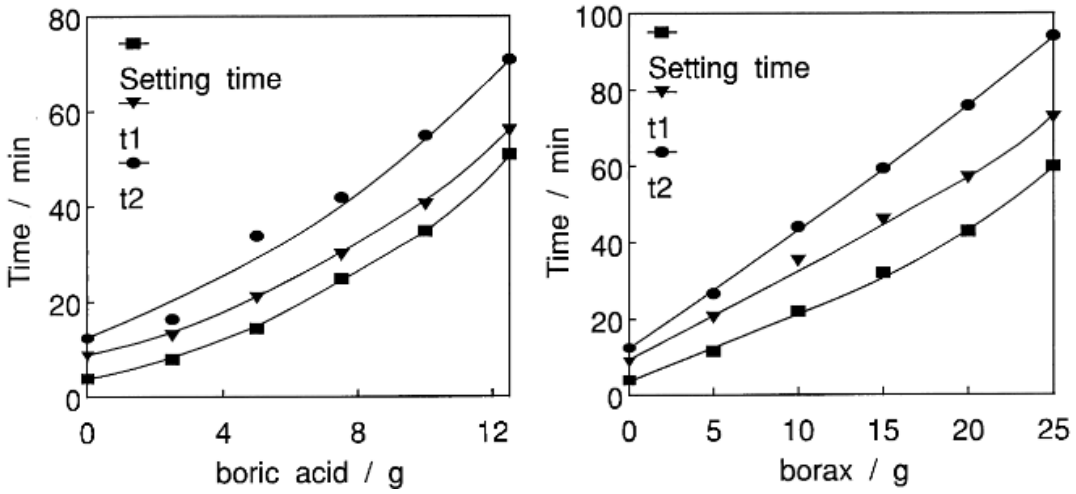


Figure 2.9 Effect of different retarders on setting time of the MPC mortars (Hall et al., 2001)

Mixture design can also change the setting time. By increasing M/P, the acid and base components react in a shorter time and setting happens faster (Figure 2.10). Also, increasing W/B can increase the setting time (Figure 2.11) since more water reduces the ability of the acidic ions to react. (Bilginer & Erdoğan, 2021; Li & Chen, 2013)

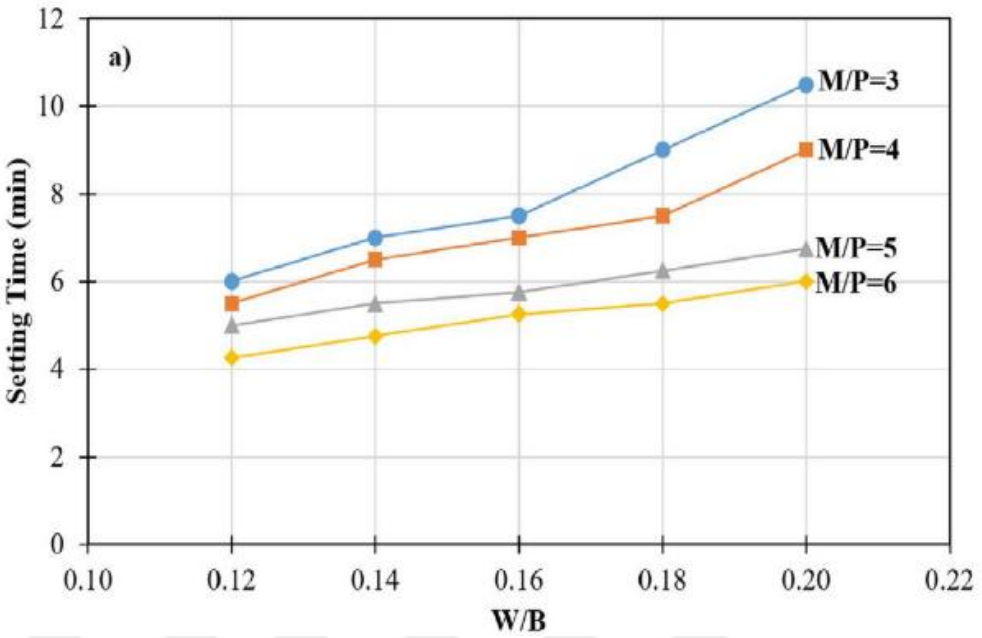


Figure 2.10. Influence of M/P on the compressive strength of MPC pastes (Bilginer & Erdoğan, 2021)

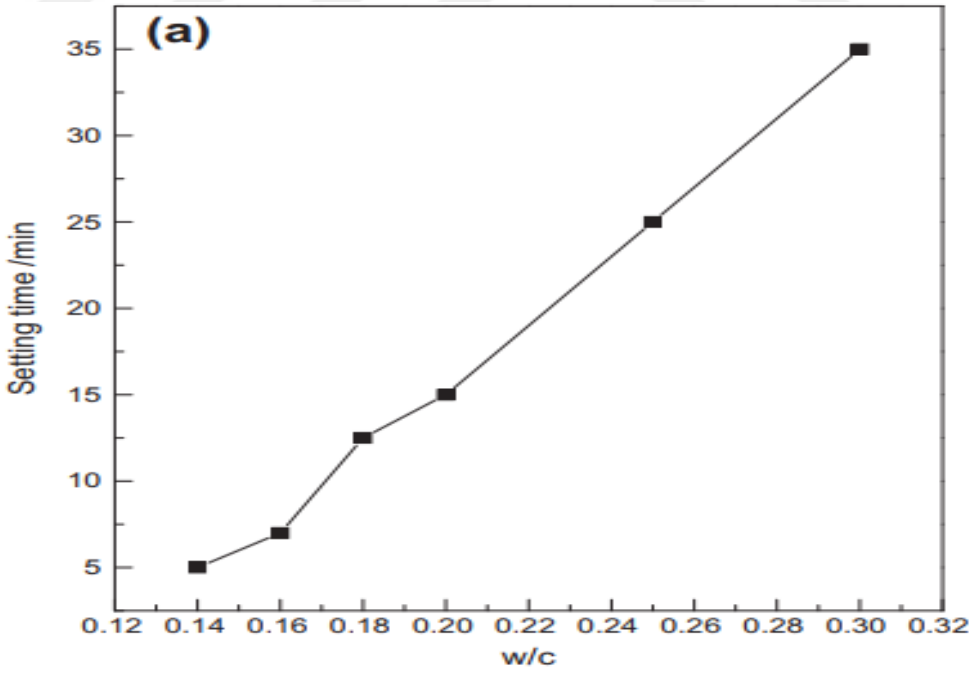


Figure 2.11. Effect of W/B (W/C in this study) ratio on the setting time of MPC pastes (Li & Chen, 2013)

2.1.1.4 Major Drawbacks of Magnesium Phosphate Cement

Despite all its advantages, magnesium phosphate cement has some major drawbacks. As shown previously, setting time in some cases is less than 5 minutes, making it hard to work with, and even a high amount of retarder isn't helpful because it reduces early compressive strength. Also, in MPC mixes without any additives, compressive strength decreases significantly after immersing in water compared to samples cured in air, and this is because the final products, struvite, and K-struvite, dissolve at low pH and reduce the compressive strength of the sample (Li et al., 2016). Further, the reactions in MPC have very high hydration heat that dramatically raises the temperature of MPC pastes (Figure 2.12). In comparison, Bentz (2010) observed that the highest temperature reached in a hydrating Portland cement paste is around 50 °C for a 330 g sample.

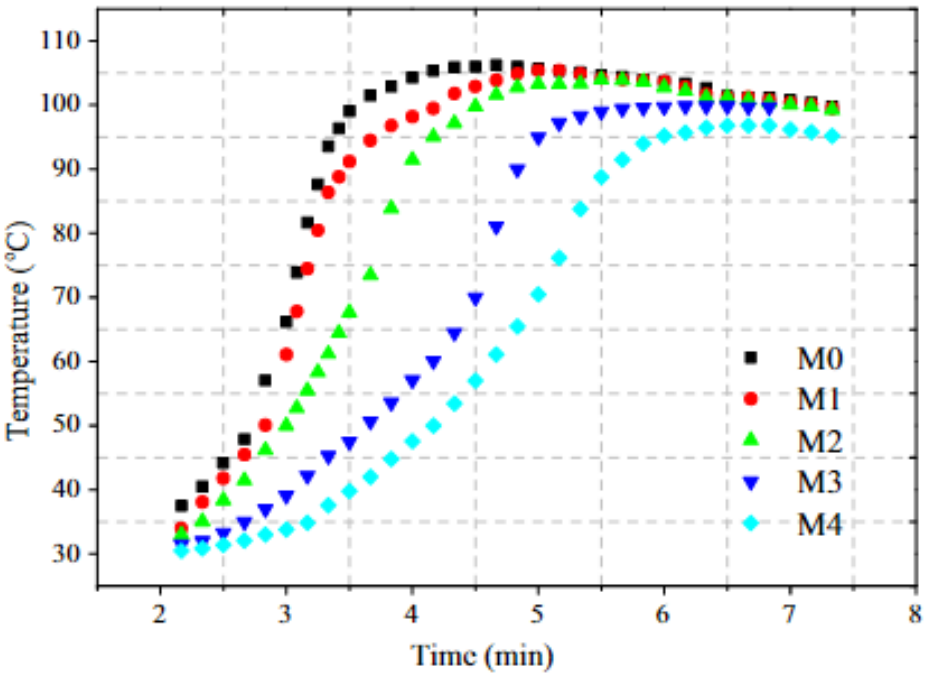


Figure 2.12. Temperature evolution of MPC mixes with and without alumina. Alumina content is increased from M1 to M4 (Liu & Chen, 2016). All the samples have a constant volume of 64 cm^3.

2.1.1.5 Effect of Additives and Modifications on Properties of Magnesium Phosphate Cement

2.1.1.5.1 Wollastonite

Wollastonite is a calcium silicate mineral with the formula $CaSiO_3$ (Wang et al., 2022). It has been used in Portland cement (PC) mixes and didn't react because of the high pH in PC mixtures (Kalla, 2015). However, in MPC mixes, since the pH is much lower, it reacts with KH_2PO_4 to form brushite ($CaHPO_4.2H_2O$) and hydroxyapatite ($Ca_5(PO_4)_3OH$), which increase the compressive strength as shown in Figure 2.13 (Xu et al., 2020). The filling effect of wollastonite is known to be another reason for the increase in compressive strength.

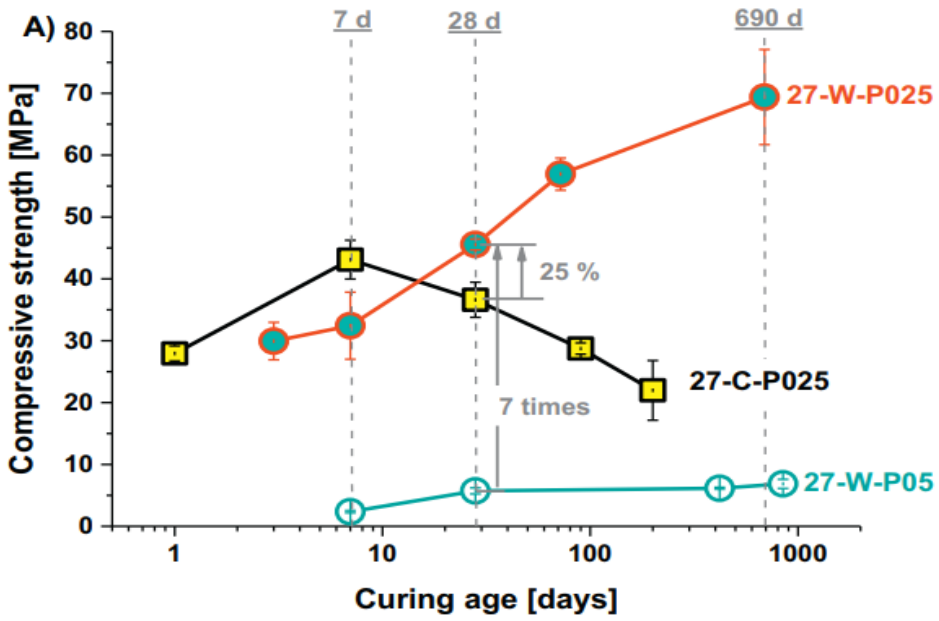


Figure 2.13. Effect of different amounts of wollastonite on MPC paste compressive strength (Xu et al., 2020). Curve 27-W-P025 shows the mixes with wollastonite and W/B = 0.25, 27-C-P025 shows the mix without wollastonite and W/B = 0.25, 27-W-P05 is for mix with wollastonite and W/B = 0.5. In all mixes, 20 % wollastonite is added.

2.1.1.5.2 Usage of Fly Ash, Steel Slag, and Silica Fume in MPC

The influence of industrial by-products, such as fly ash (FA), steel slag (SS), and silica fume (SF), on MPC has been studied. Fly ash is a by-product of the coal industry that can be used in MPC mixes. Different results can be obtained depending on the fineness and chemical composition of different fly ashes. Figure 2.14 shows that with an increase in fly ash amount, compressive strength decreases at early ages. This strength reduction can be explained by minerals in fly ash that contain oxides like SiO_2, Al_2O_3, and Fe_2O_3, which are less reactive than MgO, so they participate in the reaction at later ages and increase later compressive strength, at replacement levels up to 50 % by mass (Li & Chen, 2013). However, another study (Bilginer & Erdoğan, 2021) observed that higher than 10 % fly ash could adversely affect compressive strength even at a late age (Figure 2.15).

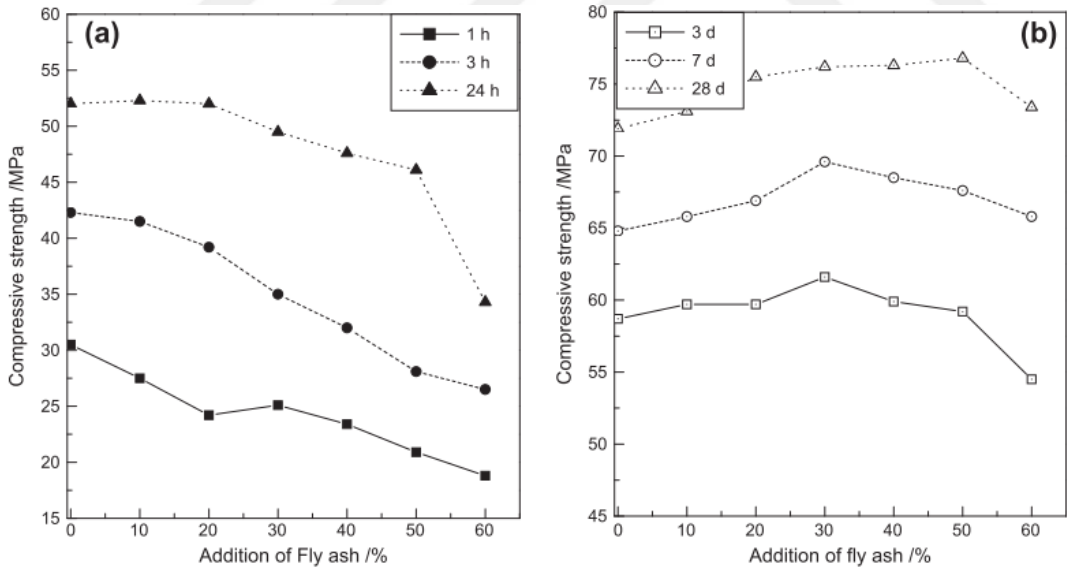


Figure 2.14. Effect of fly ash content on the compressive strength of MPC mortars (Li & Chen, 2013).

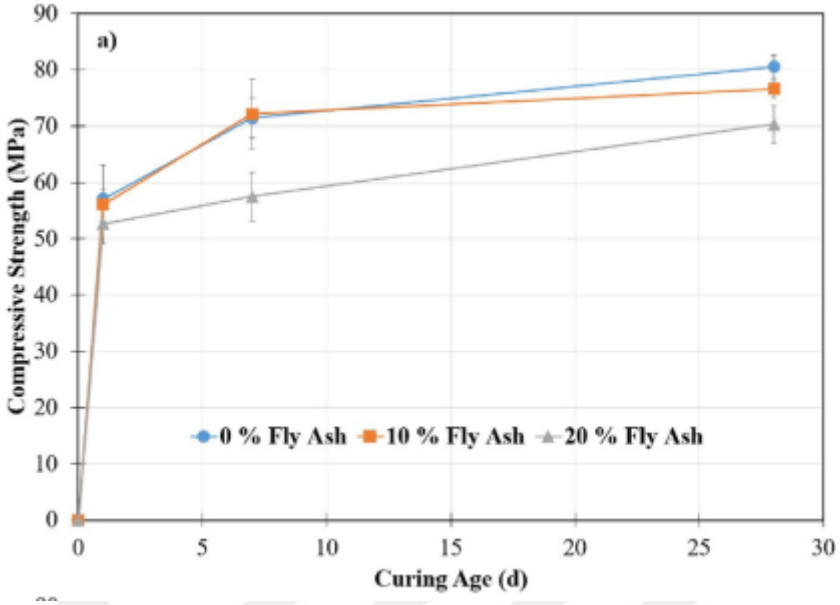


Figure 2.15. The adverse effect of fly ash on the compressive strength of MPC (Bilginer & Erdoğan, 2021)

In steel production, for each ton of steel produced, 150 kg of SS is produced as a by-product (Mo, 2018). The addition of SS in MPC mixes has been shown to improve compressive strength and resistance to water (Figure 2.16). This can be explained due to a few effects. First, SS has a filler effect, which reduces cracks and pores. Second, in water, the leaching of phosphates from dissolving k-struvite causes a reduction in compressive strength. However, in the presence of SS, the alkalinity of the system is increased, which helps the resistance of the sample in water (Ruan et al., 2022).

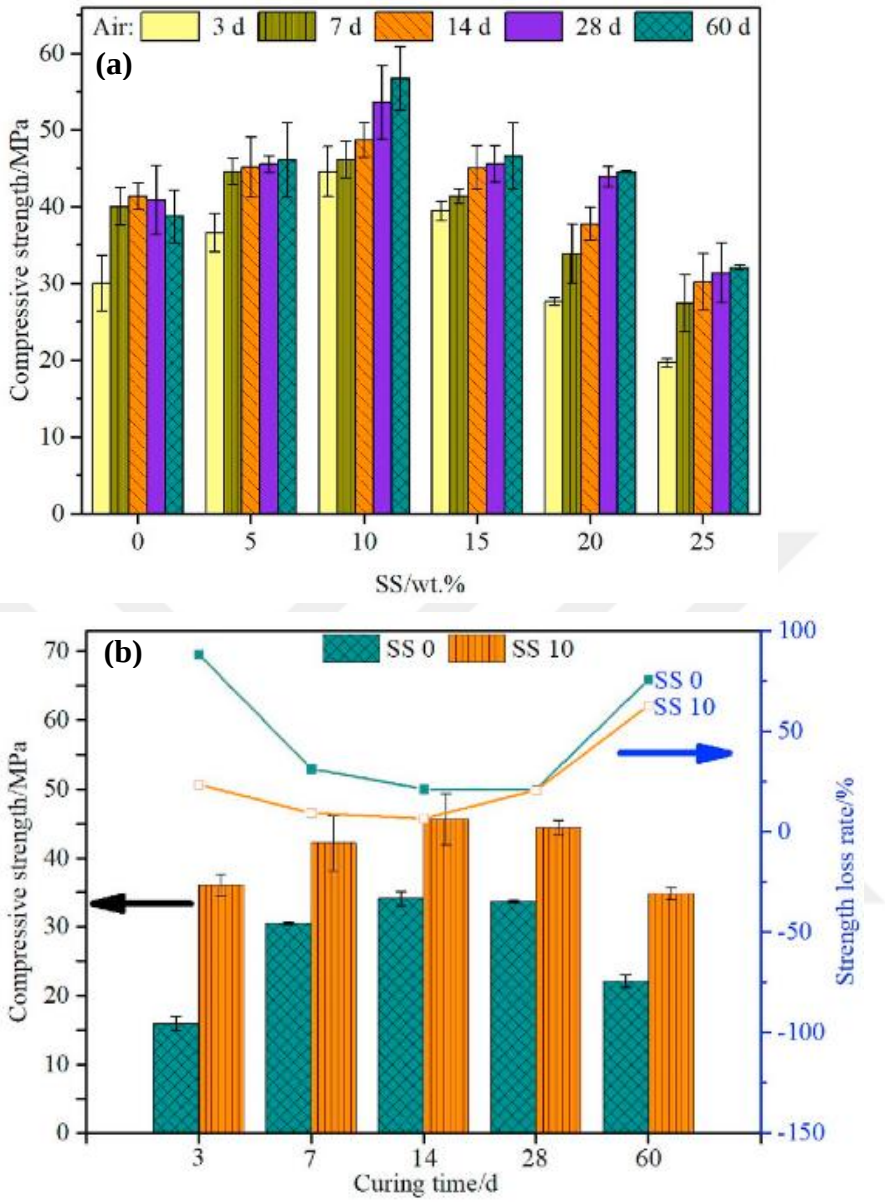


Figure 2.16. Effect of SS: a) on compressive strength b) on the water resistance, of MPC paste samples (Ruan et al., 2022)

In addition, some researchers studied using SF and FA together. As shown in Figure 2.17c, improvements can be seen in some cases when the sum of SF and FA reaches 30 %. Whereas, when the sum of these by-products increases to 40 %, there is no improvement in the compressive strength of MPC samples (Feng et al., 2022).

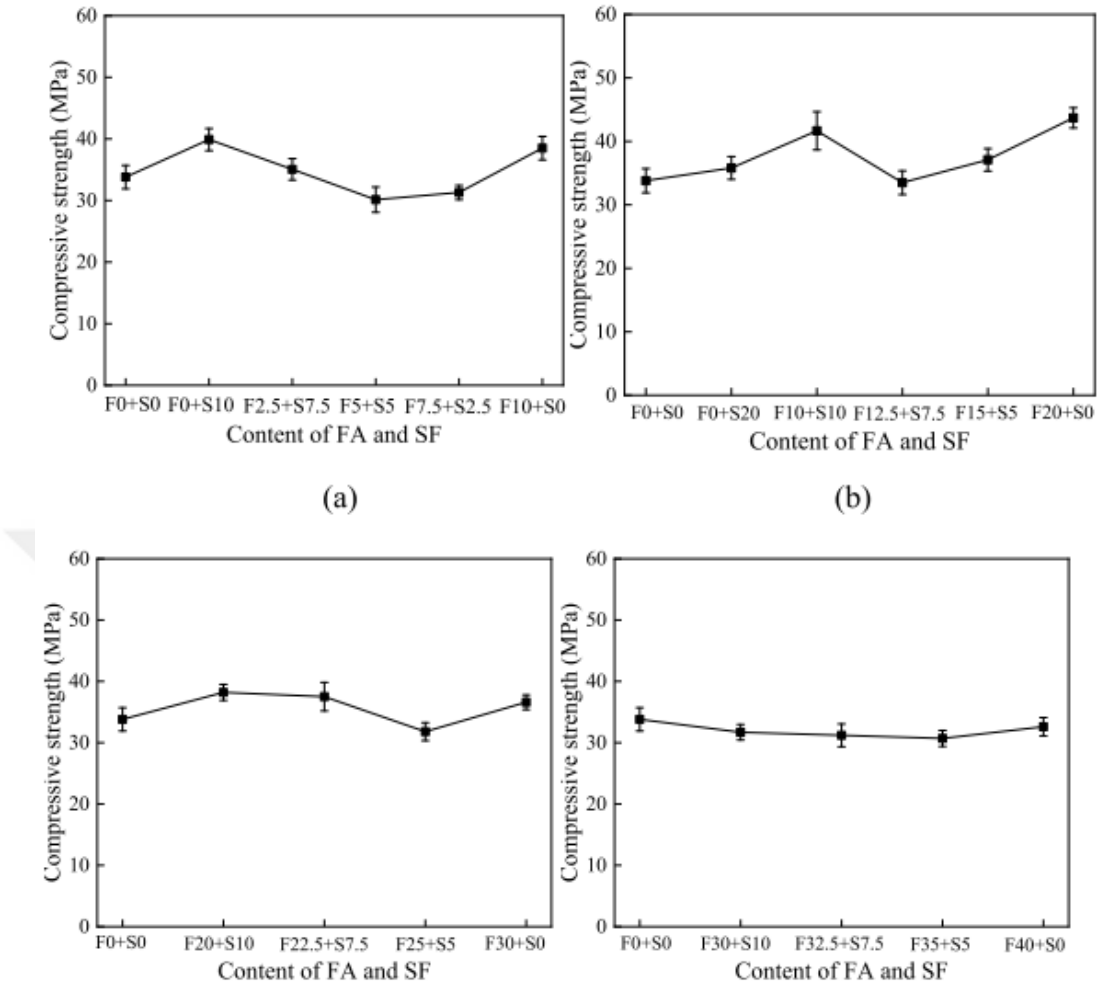


Figure 2.17. Effect of the total content of FA and SF: a) 10 %; b) 20 %; c) 30 %; d) 40 % on compressive strength of MPC (Feng et al., 2022)

2.1.1.5.3 Aluminum-Containing Materials

Aluminum is the third most abundant material in the earth's crust, and it has been observed that incorporating this element into MPC can improve its properties (Liu et al., 2020). Therefore, different materials containing a significant amount of Al_2O_3 have been studied for use in MPC. Ferroaluminate cement (FAC), a kind of sulfoaluminate cement, is such a material with more than 25 % Al_2O_3. Up to 40 %

replacement of MgO with FAC can increase compressive strength by 35 %, and 50% replacement elongates setting time from 15 minutes to 25 minutes (Figure 2.18).

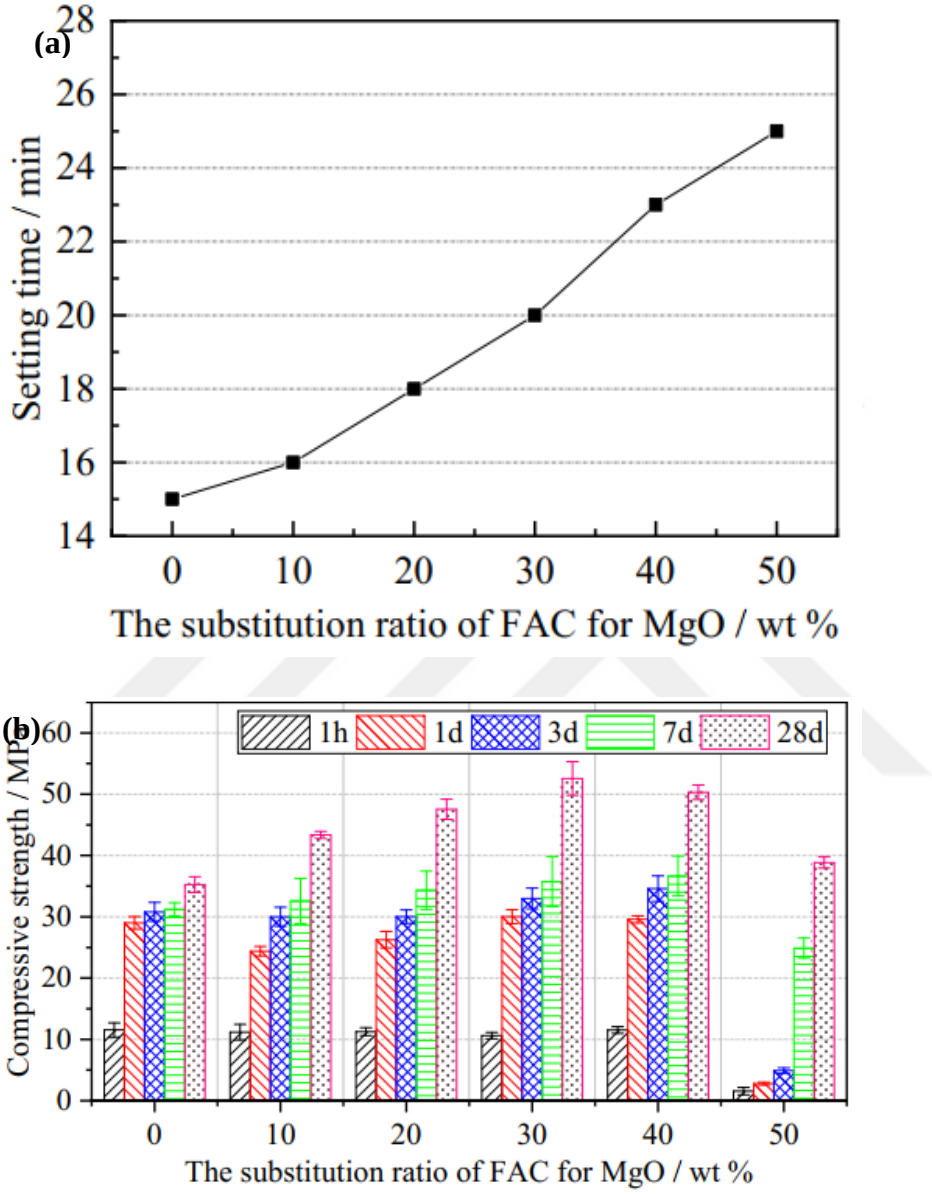


Figure 2.18. Effect of replacement of MgO with FAC on: a) the setting time; b) the compressive strength, of MPC (Jia et al., 2019)

Bauxite and red mud are other sources of Al_2O_3. Albeit, bauxite has different grades based on how much Al_2O_3 it contains. As shown in Figure 2.19, replacing MgO with

low-grade (lower Al-containing) bauxite in different percentages has increased compressive strength. Also, it increased the setting time from 13 minutes to 26 minutes (Liu et al., 2020).

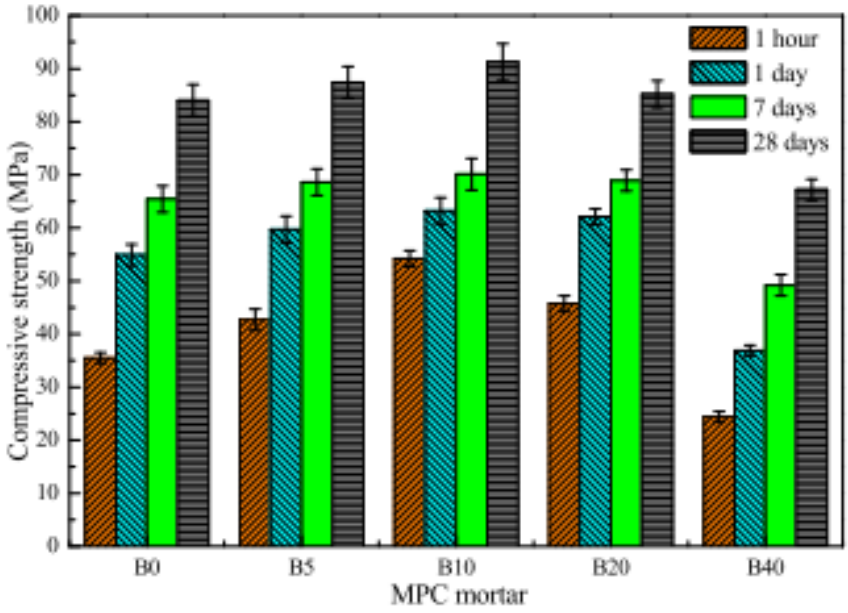


Figure 2.19. Influence of low-grade bauxite on the compressive strength of the MPC mortar samples (Liu et al., 2020)

2.1.1.5.4 Dolomite-Bauxite-Gypsum Clinkers

Dolomite is more abundant than other sources of MgO, like magnesite ($MgCO_3$). However, the presence of CaO in dolomite can be challenging because it has a higher solubility than MgO (Singh, 2001). Yu et al. (2020) used bauxite and gypsum in the calcination process of dolomite to convert CaO to ye'elimite ($Ca_4Al_6O_{12}(SO_4)$). This clinker is called a dolomite-bauxite-gypsum clinker (DBG).

Using this clinker elongated the setting time from 13 min in mixes with only MgO to 52 min with DBG calcined at 1300 °C. Also, the compressive strength was comparable with mixes made by MgO, and immersing in water after curing in air for 7 d, didn't decrease the 28 d and 56 d compressive strengths but increased it (Figure 2.20). Hydration of ye'elimite and the greater density of the sample can be the reasons

for this improvement, as new phases were not detected in the XRD results, but some amorphous structures were seen in the SEM images.

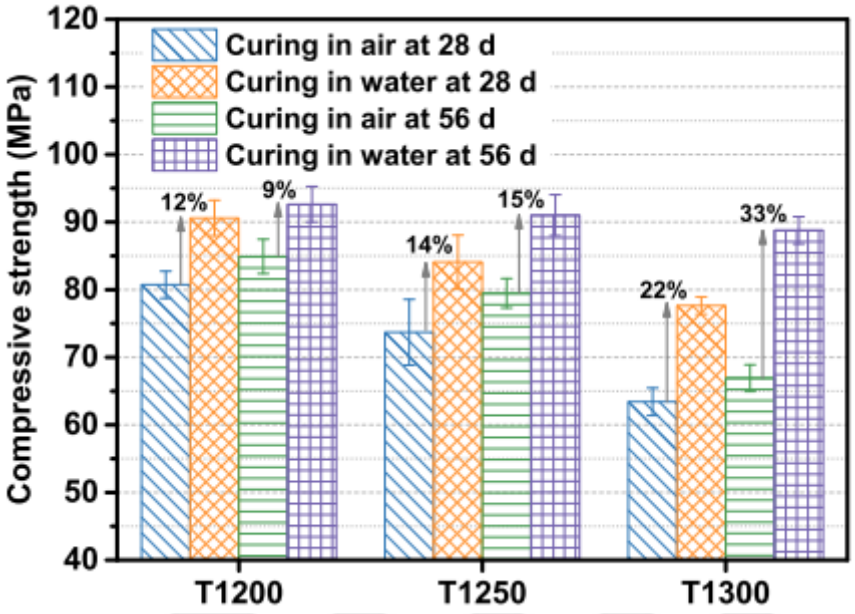


Figure 2.20. Changes in the paste compressive strength of DBG produced at different calcination temperatures (T1200: 1200 °C, T1250: 1250 °C, T1300: 1300 °C) and cured in different conditions (Yu et al., 2020)

2.1.1.6 Applications of Magnesium Phosphate Cement

Other than medical applications, MPC has been used in different areas because of its high early strength and near-neutral pH. For instance, MPC has shown acceptable performance as a road repair material. This material consumes less time and energy for repair in comparison to other materials (Li et al., 2014). Also, it has an excellent bond with ordinary portland cement (Qiao et al., 2010), making it an applicable material for repairing structures. On the other hand, some properties of MPC, like chemical stability and high bonding strength, make it a favorable candidate for waste treatment like heavy metals, and even radioactive elements (Zhang et al., 2021)

CHAPTER 3

MATERIALS AND EXPERIMENTAL PROCEDURE

This chapter discusses the raw materials used in this research as well as the experimental methods employed.

3.1 Materials

Dead-burned magnesium oxide and monopotassium dihydrogen phosphate (KH_2PO_4) were used in powder form to prepare the reference MPC mix. Also, the preparation of "fly ash phosphate", a mixture of fly ash and phosphoric acid used to supply phosphate to the solution at a controlled rate, and the production of calcium sulfoaluminate cements are explained. These two materials are used to replace magnesium oxide and monopotassium dihydrogen phosphate in MPC.

3.1.1 Dead-Burned Magnesia Powder

Magnesium oxide was ordered from Kimya Borsası in Turkey. It is white-pink in color, and its oxide composition was obtained using semi-quantitative X-ray fluorescence spectroscopy (XRF) at METU Central Laboratory (Table 3.1). This magnesium oxide is "low grade" and contains forsterite as an impurity. Bilginer & Erdoğan (2021) used a similar MgO and reported that calcination at 1500 °C reduces the reactivity of MgO significantly. In this study, the same temperature is chosen. This powder was calcined in a furnace (Protherm MoS-B 160/8), and the temperature was increased by 10 ℃/min and then kept for one hour at 1500 ℃. After calcination, the hard mass was ground in 3 kg batches for 45 minutes in the laboratory ball mill so that 90 % passes through the ASTM No. 100 sieve.

3.1.2 Fly Ash

Fly ash is used to mix with phosphoric acid to produce "fly ash phosphate" to replace KH_2PO_4 as a phosphate source in the mixes. Fly ash from Çatalağzı Thermal Power Plant was available in the laboratory. It has a grayish color, and its oxide composition is shown in Table 3.1.

Table 3.1 Oxide composition of reactive magnesium oxide and Çatalağzı fly ash

Oxide (%)	Raw Magnesium Oxide	Fly ash
MgO	86.40	1.75
SiO_2	11.10	53.50
Al_2O_3	0.06	27.90
Fe_2O_3	0.38	6.89
CaO	1.74	1.97
SO_3	0.06	0.29
NiO	0.17	0.02
P_2O_5	-	0.16
TiO_2	-	1.43
MnO	0.08	0.01
V_2O_5	-	0.07
K_2O	-	5.22
Sum	99.92	99.20

This fly ash is sieved through the ASTM No.100 sieve, and according to ASTM C 618 (2022), it is classed as a class F fly ash since its CaO content is lower than 10 %.

3.1.3 Monopotassium Dihydrogen Phosphate

As a phosphate salt to be mixed with the basic component of the acid-base cement, monopotassium dihydrogen phosphate with 99 % purity was obtained from Balmumcu Kimya in Turkey. It has coarse grains, and its solubility is 25 g/100 cm^3 water with a molar mass of 136.086 g/mol.

3.1.4 Phosphoric Acid

H_3PO_4, orthophosphoric acid, also known as phosphoric acid, was obtained from Aklar Kimya in Turkey, with an 85 % concentration. It has a density of 1.68 g/cm^3 and is used to mix with fly ash to produce fly ash phosphate.

3.1.5 Borax

Sodium tetraborate decahydrate ($Na_2(B_4O_5(OH)_4).10H_2O$), known as borax, is used as a retarder in the mixes. This powder is purchased from Balmumcu Kimya in Turkey.

3.1.6 Aggregate

The aggregate in the experiments was obtained from Santoz Sanayi Tozları in Turkey with specific gradation of 2-3 mm, 1-2 mm, 0.5-1 mm, 0.2-0.5 mm, and 0.1-0.3 mm. A mixture of these sands was used to get the gradation that is allowed in ASTM C33 (2018) as standard sand. The sieve analyses of each group of sands and the mixed sand are shown in Table 3.2. Also, the final gradation of sand obtained by mixing different sand groups and its comparison with the lower and upper boundaries in the standard are shown in Figure 3.1.

Table 3.2 Cumulative passing (%) sieve analyses of sands and their mixture

Sand size / ASTM Sieve	2-3 mm	1-2 mm	0.5-1 mm	0.2-0.5 mm	0.1-0.3 mm	Mix
No. 4	100.0	100.0	100.0	100.0	100.0	100.0
No. 8	25.2	93.1	100.0	100.0	100.0	87.4
No. 16	0.9	19.8	94.3	100.0	100.0	64.1
No. 30	0.0	1.7	16.7	99.7	100.0	37.3
No. 50	0.0	0.7	4.7	48.6	100.0	26.2
No. 100	0.0	0.2	0.0	1.4	22.9	4.3
No. 200	0.0	0.0	0.0	0.00	0.0	0.0

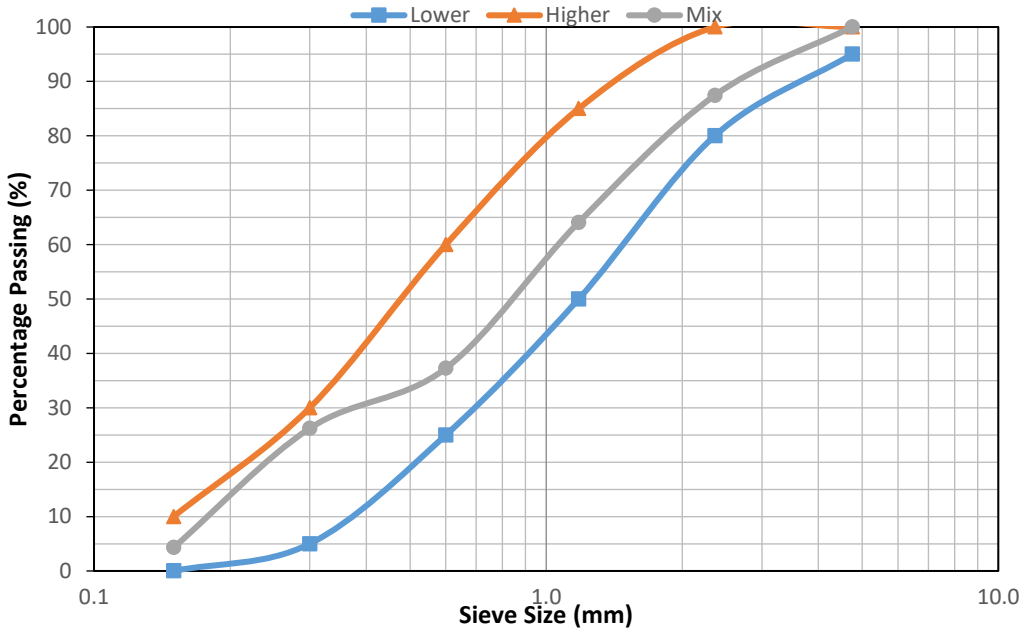


Figure 3.1 Obtained standard sand gradation compared with the ranges allowed in ASTM C33 (2018).

3.1.7 Calcium Sulphoaluminate Clinker

This thesis aimed to use calcium sulphoaluminate cement ($C\overline{S}A$) to replace MgO. The main reason is that $C\overline{S}A$ has a lower carbon footprint than MgO (Hanein et al., 2018; Luong et al., 2018). Production of this cement requires 1300 ℃, which is lower than the magnesium oxide calcination temperature (1500 ℃). Typical raw materials used in calcium sulfoaluminate clinker production are bauxite, limestone, and gypsum. Also, clay is added in the production process as a raw material to change the composition of clinker and study its influences. Clay is a less expensive and more environmentally-friendly material, and it was expected to help form more belite (dicalcium silicate) to reduce the reactivity of the clinker and elongate the setting time. Limestone, gypsum, and clay were available in the laboratory, and bauxite was obtained from Demireller Mining in Turkey. Each of the materials was ground to pass the No.100 sieve and their oxide compositions are shown in Table 3.3.

Table 3.3. Oxide composition of raw materials for clinker

Oxide Content (%)	**Bauxite**	**Limestone**	**Gypsum**	**Clay**
Al_2O_3	50.00	1.73	0.73	19.10
Fe_2O_3	13.70	1.21	0.51	6.39
SiO_2	13.40	3.91	1.90	56.20
TiO_2	3.41	0.12	0.06	1.15
CaO	2.52	48.10	31.20	3.76
K_2O	1.27	0.30	0.11	2.30
MgO	0.49	1.14	0.19	2.72
Na_2O	0.25	-	-	0.46
MnO	0.15	0.04	0.02	0.25
ZrO_2	0.11	-	-	0.03
SO_3	-	-	52.80	1.08
L.O.I*	13.90	46.70	13.64	6.00
Sum	99.40	99.85	99.87	99.44

*Loss on ignition

Twelve clinkers were designed with different raw material proportions (Table 3.4). Canbek & Erdoğan (2020) reported C1 in Table 3.4 could be considered a "reference calcium sulphoaluminate cement" and suggested 1300 ℃ as the calcination temperature. In C2, limestone content is decreased and other components are increased to reduce CO_2 emissions since limestone has a high loss on ignition. In C3, clay is added to partially replace bauxite and limestone, because clay is less expensive and has lower L.O.I. C4 aims to investigate the influence of the higher amount of clay in comparison to C3. C5 is similar to C3, only the content of clay is increased, and limestone is reduced. C6 is similar to C4, the content of gypsum and bauxite is kept constant, but the amounts of clay and limestone are changed. C7-C12 were designed to obtain clinkers with no or low amounts of bauxite since it is an expensive material. However, C7-C12 melted at 1300 ℃, so it was impossible to use them any further (Figure 3.2).

Table 3.4. Raw materials proportions (%) of $C\overline{S}A$

Clinker	Limestone	Clay	Gypsum	Bauxite
C1	40.00	0.00	20.00	40.00
C2	30.00	0.00	25.00	45.00
C3	43.75	11.25	15.00	30.00
C4	28.00	20.00	17.50	34.50
C5	38.75	16.25	15.00	30.00
C6	34.00	14.00	17.50	34.50
C7	35.00	65.00	0.00	0.00
C8	36.25	48.75	5.00	10.00
C9	20.00	70.00	10.00	0.00
C10	30.00	60.00	10.00	0.00
C11	20.00	60.00	20.00	0.00
C12	20.00	50.00	10.00	20.00



Figure 3.2. Melted clinker (brownish part) on the furnace plate in the calcination process

Since the number of clinkers is high, preliminary compressive strength testing is performed on mortars made with these clinkers to select the ones that give the highest 24-h compressive strength, in an effort to save material, energy, and time. Mix design and results of the preliminary tests are explained in Section 3.2.4. Based on the obtained results, C1-C4 are chosen for further tests. Their calculated oxide compositions, according to Tables 3.3 and 3.4 are shown in Table 3.5.

Table 3.5. Oxide composition of selected C$\overline{S}$A

Oxide Content (%)	C1	C2	C3	C4
Al_2O_3	11.00	13.35	18.88	21.68
Fe_2O_3	6.27	7.57	10.28	11.73
SiO_2	5.00	5.38	14.95	17.29
TiO_2	0.75	0.92	1.26	1.45
CaO	30.95	27.96	23.41	19.38
K_2O	0.42	0.46	0.89	1.00
MgO	0.63	0.55	1.06	1.06
Na_2O	0.05	0.06	0.15	0.18
MnO	0.05	0.06	0.10	0.12
ZrO_2	0.02	0.02	0.03	0.04
SO_3	21.12	23.76	8.10	9.46
MnO	0.06	0.07	0.05	0.05
NiO	0.02	0.02	0.01	0.01
TOTAL	99.68	99.65	99.59	99.45

In addition, X-Ray Diffraction Analysis (XRD) is done on these four clinkers (Figure 3.3). By increasing the clay amount in C1-C3, larnite peaks are densified. However, in C4, since the clay amount is highest, the minerals formed at 1300 °C are changed from ye'elimite and brownmillerite to gehlenite and hercynite.

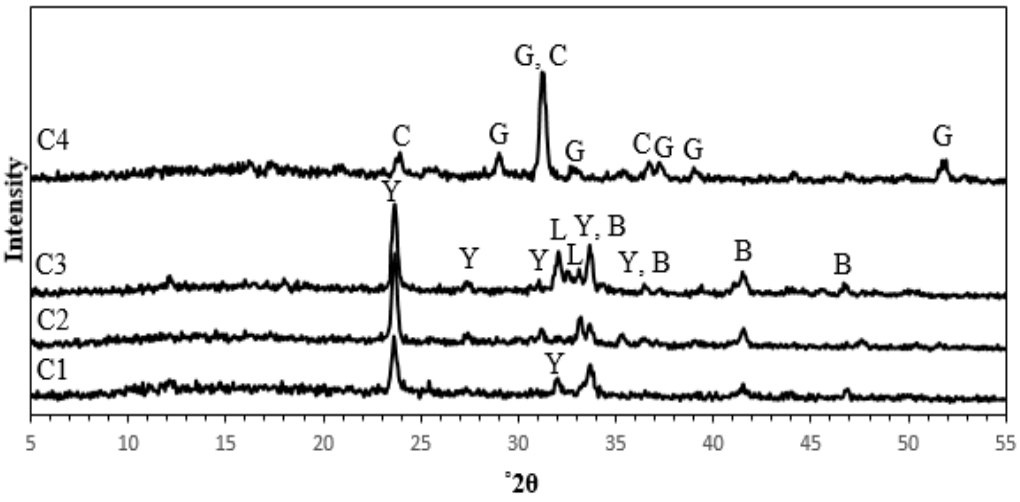


Figure 3.3 XRD results for clinkers. G: Gehlenite, C: Hercynite, B: Brownmillerite, Y: Ye'elimite, L: Larnite

Overall, using C$\overline{S}$A instead of MgO can reduce the costs remarkably, since the raw materials are less expensive and the consumed energy for preparation like calcination temperature is lower than MgO. Among the four selected clinkers, in C2, limestone is lower than C1, which reduces the CaO content and L.O.I and makes the clinkers environmentally friendly. However, this increases the content of bauxite which is an expensive material in comparison. In C3, the amount of limestone is approximately the same as in C1, but the incorporation of clay reduced the bauxite content, which makes it a less expensive clinker. Finally, C4 contains less limestone and bauxite but more clay. This clinker can be both less expensive and environmentally friendly.

3.1.7.1 Clinker Production

The raw material powders were mixed for 2 minutes in a cement mixer at low speed to get a homogenous mix. Then, water was added at 25 % by mass of the raw materials, and mixing was continued for 5 minutes. Fire bricks were used as a plate for placing clinker in the furnace because it is cheaper than other plates. A prepared

paste of raw materials is used as a foundation-like mesh shape on the brick to avoid impurities from the fire brick. As shown in Figure 3.4d, the top part, not in contact with the brick, is taken as the clinker to be used to prepare phosphate cement.

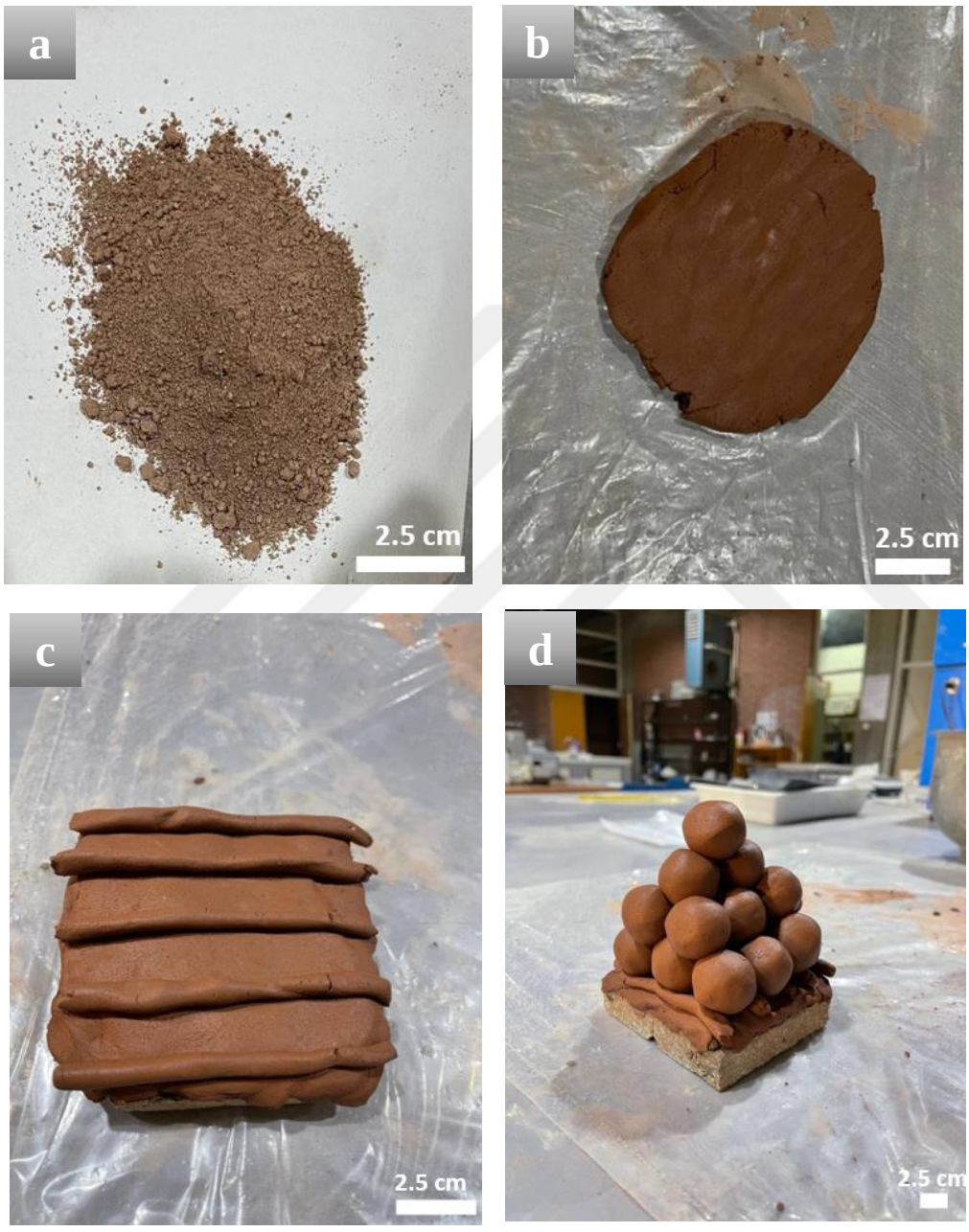


Figure 3.4. a) Powder mix of clinker raw materials, b) Paste after mixing of raw materials with water, c) Underlayer used for putting clinker paste d) Final form of clinker preparation (ball-shaped samples are used)

After calcination, the balls of clinkers were crushed into small pieces with a mortar and pestle, then ground in 250 g batches for 15 minutes at 500 rpm using a planetary ball mill (PM100, Retsch). Finally, they were sieved through the No. 100 sieve to be used in the mixes. A summary of clinker production is shown in Figure 3.5.

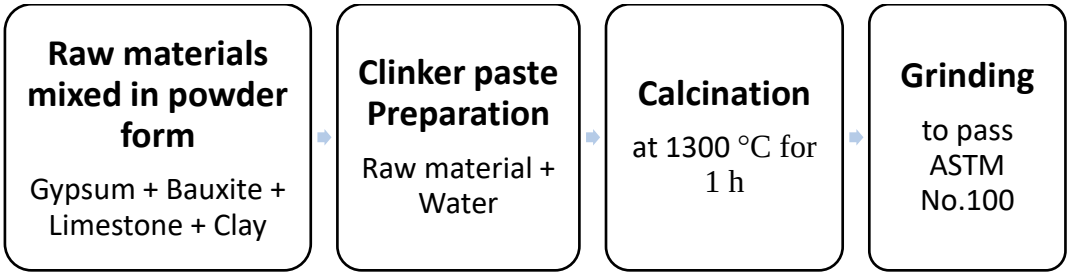


Figure 3.5. Process of clinker production

3.1.8 Fly Ash Phosphate ($FAPO_4$)

In MPC mixes, KH_2PO_4 is used as the acidic component. In this study, Çatalağzı Fly Ash is mixed with phosphoric acid to obtain "fly ash phosphate ($FAPO_4$)" to use in MPC mixes, which is supposed to increase the initial pH of the phosphate cement in comparison to the pure phosphoric acid and to have mixtures with longer setting time. Also, water is used in this process to help to mix fly ash with phosphoric acid easily. Four different ratios of phosphoric acid:fly ash:water were selected (Table 3.6) to compare with KH_2PO_4.

Table 3.6. Mix proportions for $FAPO_4$ and comparison of their PO_4 molar ratio with KH_2PO_4

Mix Label	Phosphoric Acid	Fly Ash	Water	The mass ratio of PO_4 *
$FAPO_4$-1	1.0	1.0	0.5	0.45
$FAPO_4$-2	1.0	1.5	0.5	0.36
$FAPO_4$-3	1.5	1.0	0.5	0.54
$FAPO_4$-4	1.0	1.0	1.0	0.36
KH_2PO_4	-	-	-	0.70

* assuming that the added water evaporates after putting $FAPO_4$ in the oven.

In $FAPO_4$-1, equal amounts of phosphoric acid and fly ash were used, and (50 % by mass of phosphoric acid or fly ash) water was added. In $FAPO_4$-2, the effect of more fly ash on $FAPO_4$ is investigated on the properties of samples prepared with $FAPO_4$. In $FAPO_4$-3, the H_3PO_4 content is increased to see whether a higher amount of acid increases the compressive strength with more reaction products. In $FAPO_4$-4, an equal amount of fly ash, phosphoric acid, and water are used to check how more water can affect the properties of the obtained fly ash phosphate.

3.1.8.1 Preparation of $FAPO_4$

Initially, fly ash, phosphoric acid, and water are mixed to get a homogenous mix (Figure 3.6a). Then, the obtained mixture is kept in a 100 ℃ furnace for 24 hours to promote the reactions within the $FAPO_4$ mixture and evaporate the extra water in the mix. Based on the proportions, the final product can be a paste or can be dry (Figure 3.6b). A summary of the mixing process for fly ash and phosphoric acid is shown in Figure 3.7.

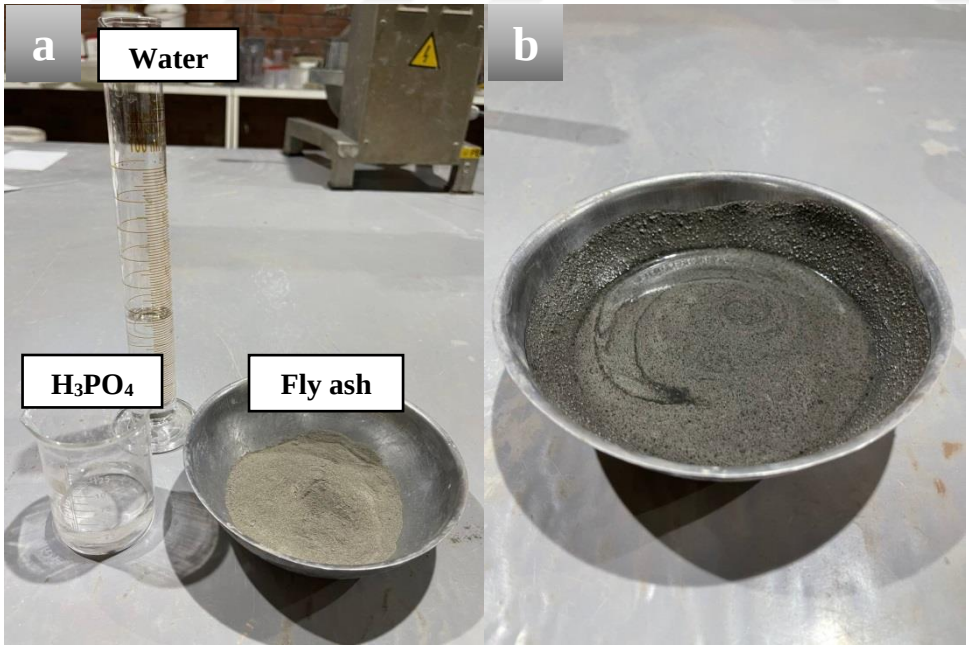


Figure 3.6. $FAPO_4$: a) Raw materials, b) After mixing the raw materials.

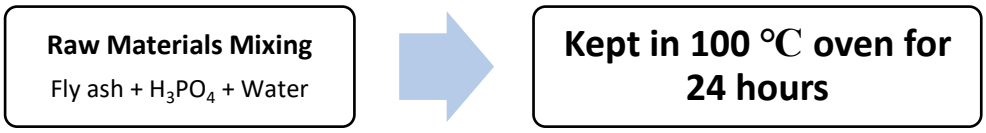


Figure 3.7. Process of $FAPO_4$ production

3.2 Experimental Procedure

3.2.1 Groups of Phosphate Cement Mixtures

The reference mix in this study is a combination of MgO and KH_2PO_4, typical for MPC mortar and paste samples. Replacement of these basic and acidic components with $C\overline{S}A$ and $FAPO_4$ is done in three groups of mixtures (Table 3.7). Group I, named MgFAz, contains MgO and different $FAPO_4$, where z is the number of FAPO4 in Table 3.6. Group II (CxKH) contains KH_2PO_4 and one of the four clinkers, where x is the clinker number in Table 3.5. In Group III (CxFAz), $FAPO_4$ and one of the clinkers are mixed to investigate the full replacement of the powders in the reference mixture.

Table 3.7 Mixture Groups

Mixture Group	Mixture Label	Components
Reference	R	MgO + KH_2PO_4
Group I	MgFAz	MgO + $FAPO_4$-z
Group II	CxKH	Cx + KH_2PO_4
Group III	CxFAz	Cx + $FAPO_4$

3.2.2 Preparation of Mortar Samples

In this study, as mentioned in Section 3.1.7, preliminary compressive strength tests were performed to determine the mix design and to select a few clinkers among the twelve in Table 3.4, to prepare standard samples. In the following sections, the preparation of preliminary and standard samples is explained.

3.2.3 Mixing Process

First, the PO_4 source (KH_2PO_4 or $FAPO_4$) and borax are mixed with water. Then, sand is added in two equal parts. In the end, magnesium oxide or clinker is added, and mixing continues for 30 seconds in mixes made with $FAPO_4$ (Group I and III), or for 4 minutes in mixes made with KH_2PO_4 (Group II). The order of mixing is illustrated in Figure 3.8. Mixing is done with a spoon, and samples are cast in two layers. The mold is tapped on the table 30 times in 20 seconds for each layer. Plexiglass molds have been used instead of metal ones because they facilitate demolding without using oil.



Figure 3.8. Mixing process for preparing mortars

3.2.4 Preparation and Compressive Strength of Preliminary Samples

Preliminary compressive strength tests were performed on 2.5 cm cubes before the standard tests (Figure 3.9). This is done to choose some successful mixture designs to continue with standard compressive strength tests (5 cm cubes). The mixture design used in each group of mixtures and their compressive strength are shown in Tables 3.8-3.10.

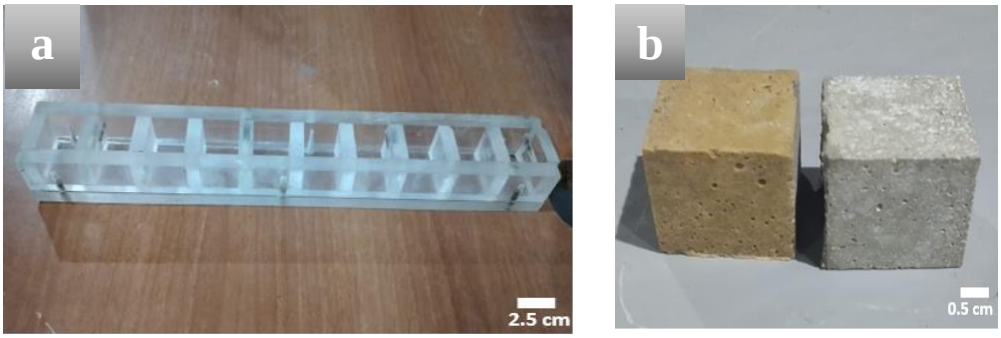


Figure 3.9. Cubes with 2.5 cm sides: a) Mold used for preliminary tests; b) Prepared samples.

Table 3.8. Preliminary mixtures of MgFAz (Group I)

Mixture	W/B	S/B	$MgO/FAPO_4$ (mass ratio)	Borax (mass % of MgO)	24-h Compressive Strength (MPa)
P*-MgFA3-1	0.30	2	0.6	5	14.6
P-MgFA3-2	0.22	2	0.6	5	17.6
P-MgFA3-3	0.22	2	1.0	5	27.3
P-MgFA3-4	0.22	2	1.5	5	38.7
P-MgFA3-5	0.20	2	1.5	5	41.5

* P indicates a preliminary test

In MgFAz mixes (Group I), only $FAPO_4$-3 is used for preliminary samples, and when $MgO/FAPO_4$ is equal to 0.6 and W/B is reduced from 0.30 to 0.22, an increase in compressive strength is observed. However, even this higher compressive strength is lower than the strength of comparable mortars in the literature. So, one possible way to increase the strength is to increase $MgO/FAPO_4$, to get more products. The mixing process is difficult when this ratio reaches 2 since it is done with a spoon in a short time. Therefore, $MgO/FAPO_4$ ratio is selected as 1.5 for these mixes. Also, different W/B's have been tested to select the lowest W/B for $MgO/FAPO_4$=1.5, which still gives a workable mixture. When W/B is reduced to 0.18, the mix becomes dry and hard to cast. Therefore, W/B=0.2 is selected, and S/B is chosen as 2 because it reduces the contact surface of particles, which gives more time to cast, and reduces the usage of binders for the same volume.

Table 3.9. Preliminary mixtures of CxKH (Group II)

Mixture	W/B	S/B	MgO/FAPO4 (mass ratio)	Borax (mass % of MgO)	24-h Compressive Strength (MPa)
P-C1KH-1	0.10	1	1.0	5	14.6
P-C1KH-2	0.10	1	1.5	5	24.5
P-C1KH-3	0.14	1	1.5	5	32.4
P-C2KH-3	0.14	1	1.5	5	18.1
P-C3KH-3	0.14	1	1.5	5	38.6
P-C4KH-3	0.14	1	1.5	5	12.4
P-C5KH-3	0.14	1	1.5	5	7.7
P-C6KH-3	0.14	1	1.5	5	6.0
P-C1KH-4	0.18	2	1.5	5	16.7
P-C1KH-5	0.20	2	1.5	5	17.6
P-C1KH-6	0.22	2	1.5	5	19.7

For CxKH mixes (Group II), different clinker/KH_2PO_4 and W/B are tested. For mix P-C1KH-3 a comparable 24-hour compressive strength with literature is obtained and it is repeated for other clinkers in Table 3.4 to choose better-performed ones for standard tests. Then, to have a mix design similar to Group I, S/B is increased to 2 in mixture P-C1KH-4. With this change in S/B, the mix demanded more water to be workable. Finally, in P-C1KH-6 castable mixture could be obtained and selected as a mixture design for Group II.

Table 3.10. Preliminary mixtures of CxFAz (Group III)

Mixture	W/B	S/B	MgO/FAPO4 (mass ratio)	Borax (mass % of MgO)	24-h Compressive Strength (MPa)
P-C4FA1-1	0.30	2	1.0	5	9.8
P-C4FA1-2	0.22	2	1.0	5	13.2
P-C4FA1-3	0.22	2	1.5	5	19.3

In Group III, the tested mixtures are shown in Table 3.10. In this group, the same mix design in Group I is used and a workable mix could be obtained only with C4.

The mixtures containing C1, C2, and C3 react too rapidly to cast samples. Also, $FAPO_4$-1 is used for these mixtures.

3.2.5 Mix Design of Standard Samples

Based on the preliminary tests, a specific mix design was used in all mixes with different materials (Table 3.11) but with 10 % higher W/B in CxKH (Group II). This higher W/B was needed because the phosphate source in Group II, KH_2PO_4 is a dry powder but $FAPO_4$ in Groups I and III is a wet paste. The mass of the liquid portion of $FAPO_4$ was measured by drying 50 g of $FAPO_4$ in a 100 °C oven for 20 days and determined as 10 %.

Table 3.11. Mix design used to prepare the standard samples

Mixture Group	W/B	S/B	(MgO or clinker)/(H_3PO_4 or $FAPO_4$) (mass ratio)	Borax (mass % of clinker or MgO)
Groups I and III	0.20	2	1.5	5
Group II	0.22	2	1.5	5

3.2.6 Determination of Compressive Strength

A compressive strength test was performed on 5-cm cube mortar samples. For each mix, three samples were tested at ages 3 h, 24 h, 7 d, and 28 d. Since MgFAz and CxFAz mixes set rapidly, they were demolded after 1 hour. For CxKH, since the setting time is much longer, they were demolded 15 hours after casting. The test was performed with UTCM-6420 (UTEST) cement compression and flexural machine, and the applied force has a constant rate of 1.5 kN/s.

3.2.7 Determination of Water Resistance

Water resistance of each of the three different groups of mixes was measured using four air-cured standard mortar samples; two were tested in compression at 28 d, and the other two were immersed in water for an additional 14 days and tested at 42 d. The residual compressive strength (RCS) of mixtures is calculated as:

$$RCS = (A - W) * 100 / A \quad (3)$$

where; A is the 28-d compressive strength of air-cured samples, and W is the compressive strength after 14 additional days in water.

3.2.8 Determination of Setting Time

Setting times of the three groups of mixtures were measured according to ASTM C191 (2021) but with some changes. A 4x4 cm cylinder mold was used for this test. The mix design for paste was the same as that selected in preliminary tests in all mixtures groups (Table 3.11). For MgFAz and CxFAz (Group I and III), the depth penetration of the Vicat needle was measured every 15 s. To gain better insight about setting behavior of CxKH (Group II), the penetration depth was recorded every minute in the first 5 min, and then every 10 min until setting.

3.2.9 X-Ray Diffraction Analysis

Mineralogical analyses of samples were done with an Olympus BTX-II XRD analyzer. For this experiment, paste samples were prepared, and they were ground and sieved through the ASTM No. 100 sieve. Samples were scanned from 5-55 °2θ. This test was done on 28-d-old samples.

3.2.10 Scanning Electron Microscopy

Scanning electron microscopy was performed to study the microstructure of mixtures. This test was done on 28-d-old samples at the METU Central Laboratory. Paste samples were prepared for this experiment, and a small inner part was taken as a specimen. In addition, chemical elements present in samples are determined by energy-dispersive X-ray spectroscopy (EDS).

3.2.11 Thermal Analysis

Thermogravimetric analysis (TGA) tests were used to investigate the nature of reaction products. This test was performed on 28-d-old paste samples at METU Central Laboratory, and the temperature was increased up to 1000 ˚C at a rate of 10 ˚C/min in the N_2 atmosphere.

3.2.12 X-ray Fluorescence Analysis

Characterization of the raw materials based on their oxide compositions was done by X-Ray Fluorescence analysis (XRF) at METU Central Laboratory. The analysis was done from Fluorine to Uranium, so the device couldn't identify any carbon in samples. Therefore, their loss on ignition test was done to estimate the CO_2 amount according to ASTM D7348 and recalculate the ratios obtained for oxide compositions.

CHAPTER 4

RESULTS AND DISCUSSION

This chapter presents the results obtained from explained experiments in Chapter 3 for three groups of mixtures. The effect of the two replaced materials is discussed, and the results among the different mixtures in each group are compared.

4.1 Compressive Strength

4.1.1 MgFAz Mixes (Group I)

Among the four different MgFAz mixtures, it is observed that MgFA2 (defined in Section 3.1.9) has the lowest strength at 3 h, 1 d, 7 d, and 28 d (Figure 4.1). These low compressive strengths compared to other mixtures can be explained by the low acid-to-fly ash ratio in $FAPO_4$-2. In this case, the lower amount of acid and a higher amount of fly ash leads to an inadequate reaction between acid and base.

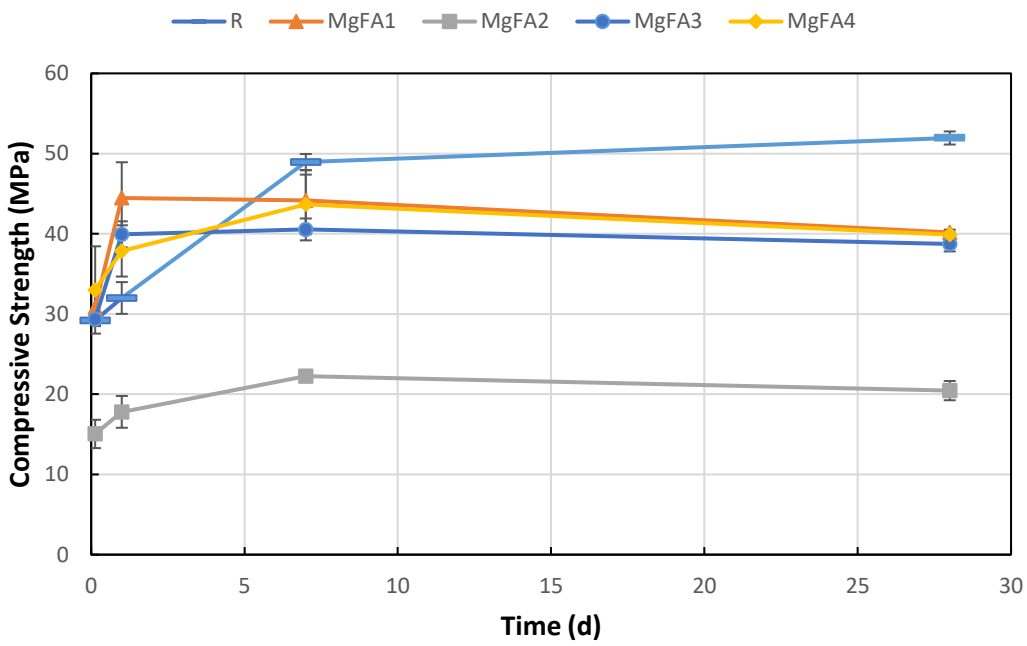


Figure 4.1 Compressive strength development of MgFAz (Group I)

The difference in the strengths of the other mixtures with varied proportions is insignificant (~2 MPa). Therefore, using more acid increases the cost of $FAPO_4$ and subsequently of the phosphate cement, and since more water is unnecessary based on the results, MgFA1 and $FAPO_4$-1 are chosen to be used for the remaining experiments. In addition, between 7d and 28 d, approximately a 10-15 % reduction in compressive strength is observed in all mixes that can possibly be related to the expansion of the unreacted MgO upon reacting with water remaining in the system.

4.1.2 CxKH Mixes (Group II)

The setting time of Group II samples is longer than 3 h, so compressive strength could not be measured at this age. In comparison, the reference mix, a magnesium potassium phosphate mortar, gained 30 MPa strength at 3 h. With time, the CxKH mixes begin and continued to gain strength, but the reference mix did not show a

significant strength increase after 7 d. C3KH has compressive strength similar to the reference at 28 d. C1KH shows an increase, but its strength is lower than those of C3KH and the reference (Figure 4.2). C2KH does not show a remarkable increase from 7 d to 28 d, which can be related to the effect of the extra water and mix design compared to the other mixtures. As observed in the preliminary tests (Section 3.2.4), these clinkers can potentially gain higher strength by optimizing W/B and S/B.

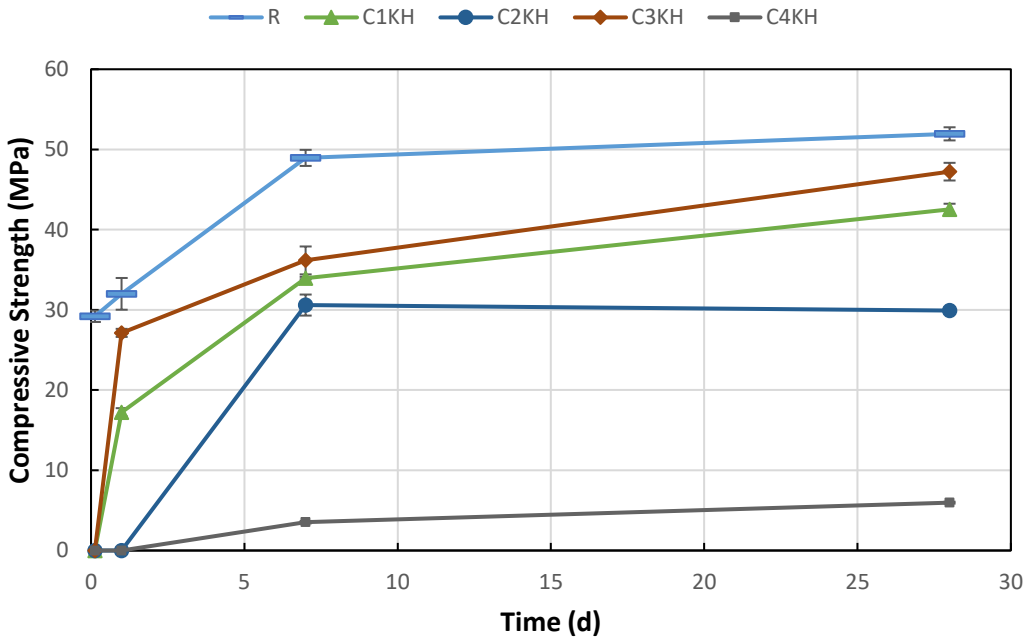


Figure 4.2 Compressive strength development of CxKH (Group II) and the reference mix

Finally, C4KH did not gain higher than 6 MPa compressive strength and was the weakest among the four CxKH mixtures. This can be explained by the presence of the highest amount of clay in this clinker (Table 3.4), which reduces the reactivity of the clinker and forms minerals that do not get in a reaction to produce strong products (Figure 3.3).

4.1.3 CxFAz Mixes (Group III)

Among the CxFAz mixes, only C4FA1 could be cast, and reactions occur quickly like in MgFAz mixes. The compressive strength of this mixture is lower than those of the reference mix or MgFAz (Figure 4.3). Like mix C4KH, the low strength of C4FA1 can be related to the minerals in this clinker (Figure 3.3), like gehlenite ($Ca_2Al(AlSiO_7)$), which have low reactivity in this system. On the other hand, at 28 d, there was no remarkable reduction in the strength of C4FA1, unlike in the MgFAz mixes (Figure 4.1).

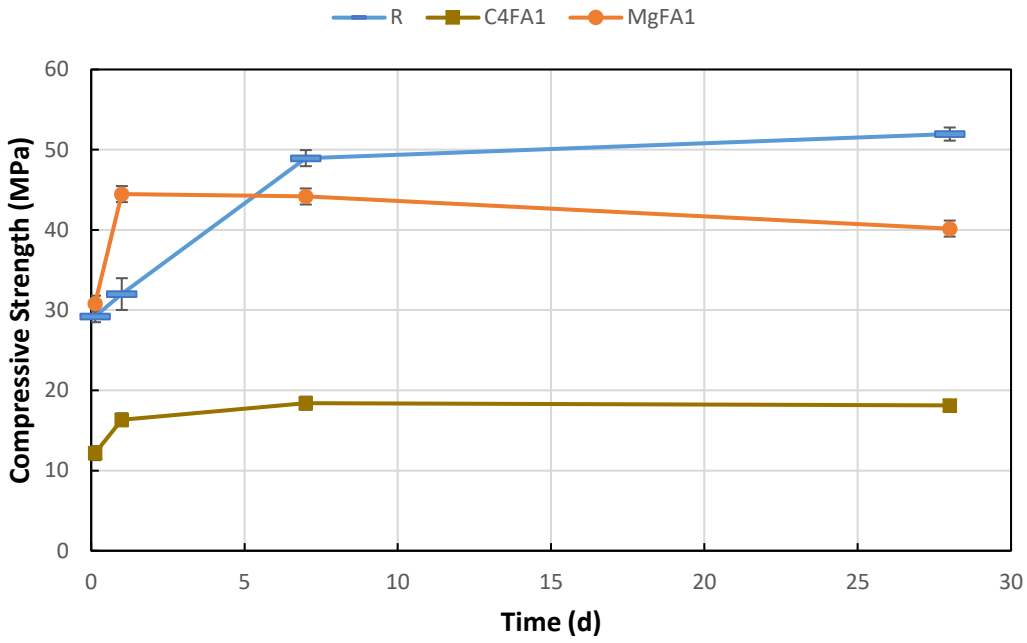


Figure 4.3 Compressive strengths development of R, C4FA1, and MgFA1

4.2 Setting Time

4.2.1 MgFAz and CxFAz Mixes (Groups I and III)

The lower initial pH in the acidic solution of Groups I and III, due to the use of $FAPO_4$ (Mahyar & Erdoğan, 2015), causes a shorter setting time than in the reference mix (~12 min). As can be seen in Figure 4.4, the setting time of the MgFA1 is about 90 seconds, but in C4FA1, the setting time extends to about 220 seconds.

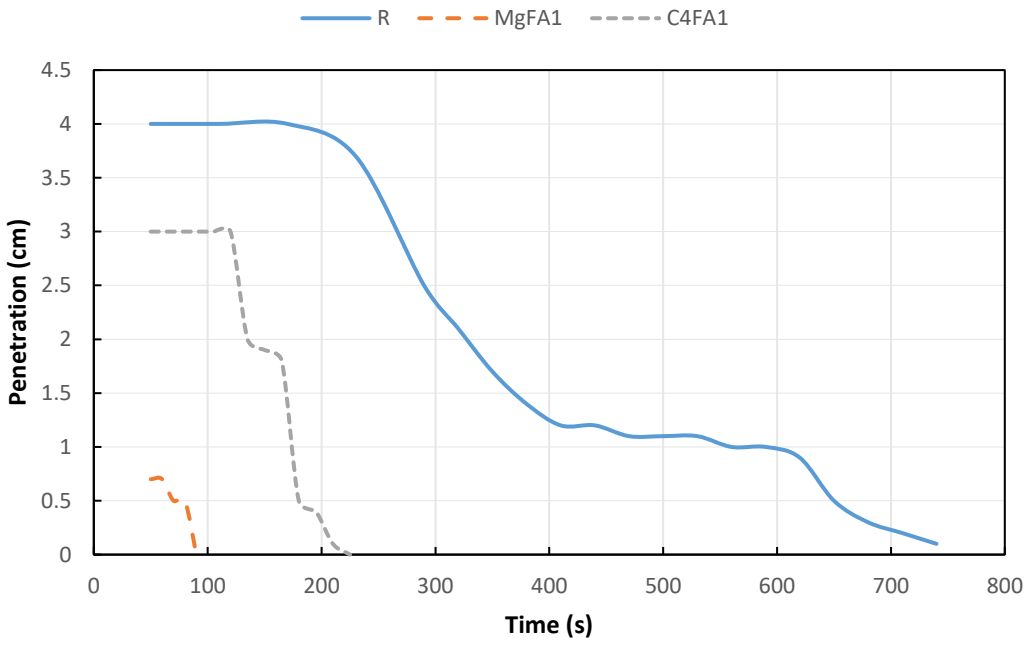


Figure 4.4. Penetration vs. time graph in setting time test of MgFA1, C4FA1, and the reference mix (Groups I and III, and R)

4.2.2 CxKH Mixes (Group II)

In the CxKH mixes, since the acid solution with KH_2PO_4 has higher initial pH than when $FAPO_4$ is used (Mahyar & Erdoğan, 2015) and the clinkers contain oxides like

CaO, which are less reactive than MgO (Table 3.5); the setting time is increased considerably from 12 minutes in the reference mix to 4-7 hours (Figure 4.5).

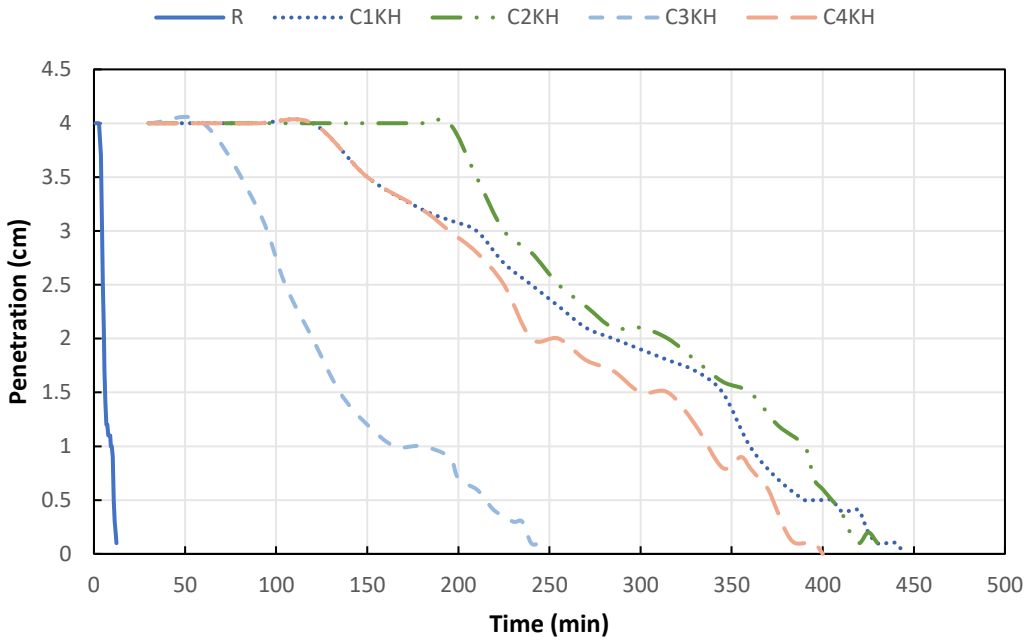


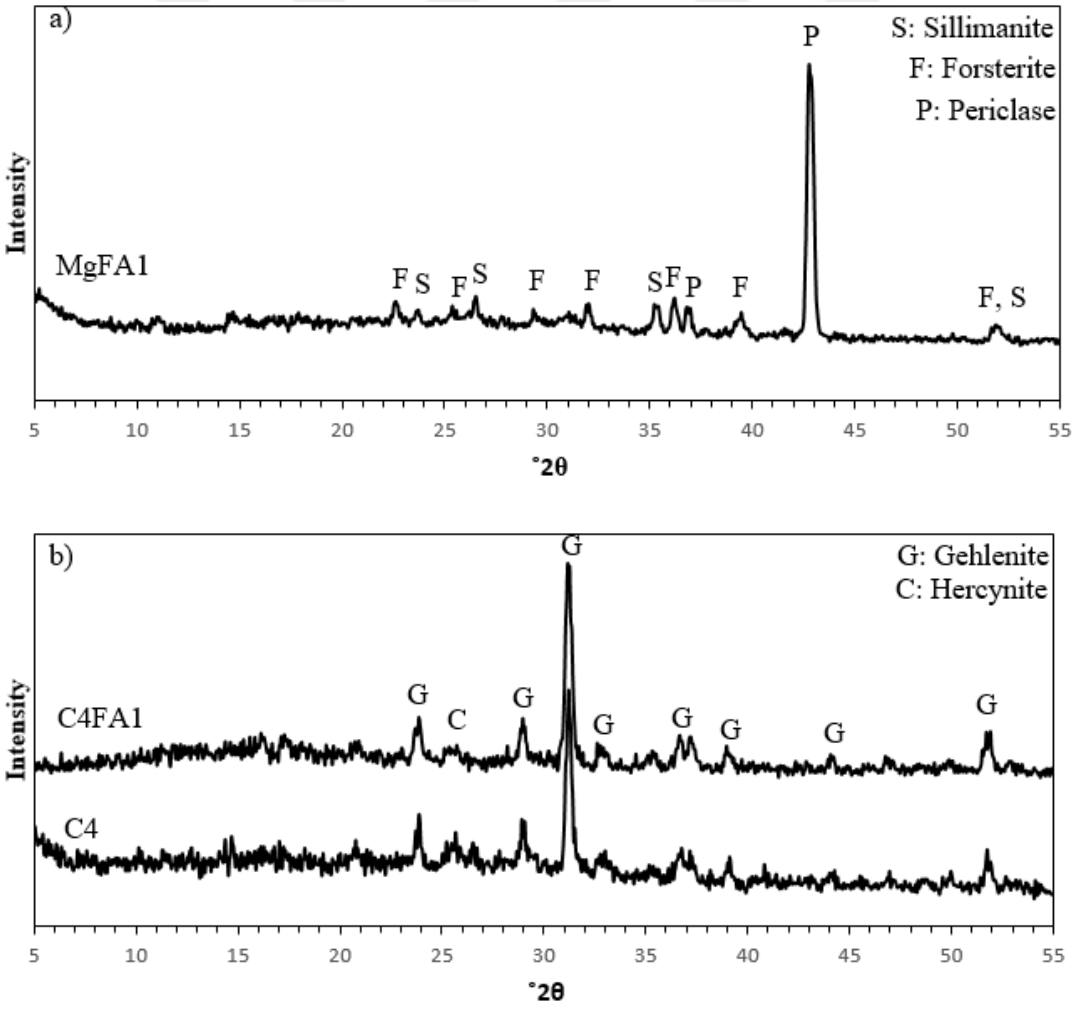
Figure 4.5 Penetration vs. time graph in setting time test of CxKH and the reference mix

As seen in Figure 4.2, C4KH doesn't gain strength higher than 6 MPa, which is quite low for a phosphate cement, so the solidification of this mix can be related to drying. The three other mixes have different raw material proportions and constant W/B, so this caused some changes in the setting time results. After C4, C3 has the highest clay amount, and C3KH had higher consistency (assessed visually). However, C1KH and C2KH which have similar setting times had lower consistency observed in the preparation process, which can be related to the greater reacting of raw minerals in C1 and C2, which were prepared without any clay.

4.3 X-Ray Diffraction Analysis

4.3.1 MgFAz and CxFAz Mixes (Groups I and III)

The XRD result of MgFA1 (Group I) is shown in Figure 4.6a. New product peaks are not visible, and all the peaks are related to the raw materials, forsterite and periclase from MgO, and sillimanite from fly ash. This suggests that any final product must be amorphous. Similarly, no product peaks are seen in the C4FA1 mix (Figure 4.6b). Peak intensities of C4 are reduced in the C4FA1 sample, which indicates the reaction of raw material but the formation of amorphous products. On the other hand, in the reference mix, K-struvite is detected, as expected (Figure 4.6c).



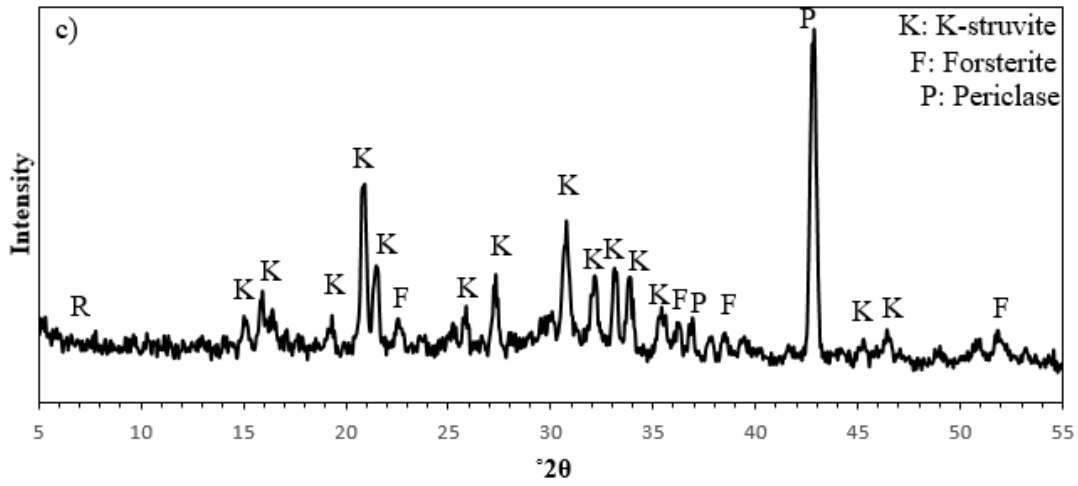


Figure 4.6 XRD result of a) MgFA1, b) C4 and C4FA1, c) Reference

4.3.2 CxKH Mixes (Group II)

Similar to the MgFA1 mixes, new peaks are not detected in the XRD diffractograms of Group II either. Figure 4.7 shows the XRD patterns of C3KH and C3. Possibly KH_2PO_4 reacts with clinker and produces amorphous products. The results for the other clinkers and mixtures are similar and are presented in Appendix A. Qian et al. (2020) have reported similar results. They reported ye'elimite in their raw material, but in the final products, there were no phases related to the reaction of ye'elimite with KH_2PO_4. Zhang et al. (2018) mixed calcium aluminate cement with KH_2PO_4 and didn't observe any hydrated calcium aluminate phases or reaction products with phosphate salt in XRD patterns. Also, in some studies related to calcium phosphate cement, amorphous products were observed (Li et al., 2014).

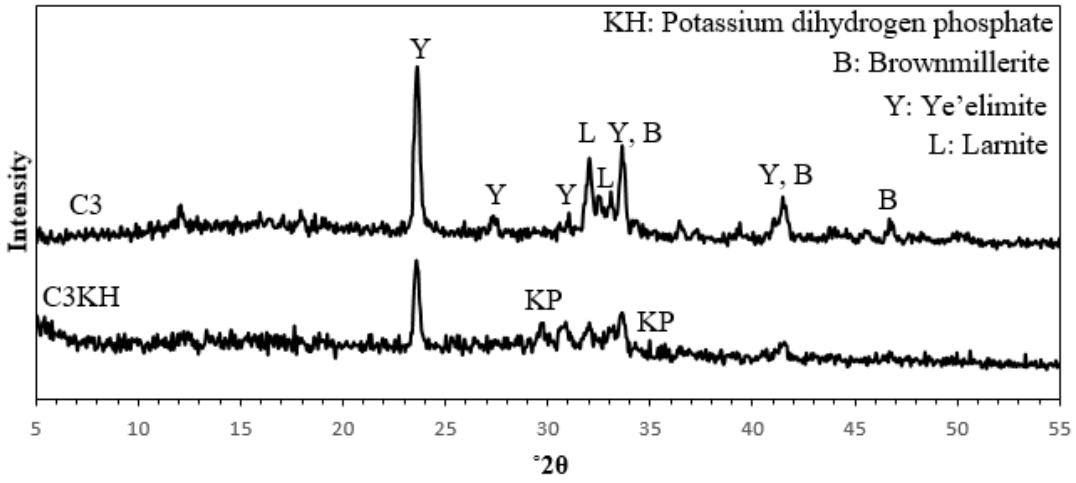


Figure 4.7 XRD pattern of C3 and C3KH

4.4 Scanning Electron Microscopy Analysis

4.4.1 MgFAz Mix (Group I)

The setting time for MgFA1 is around 90 seconds, which shows a rapid reaction and forms a porous structure (Figure 4.8a). As discussed in the XRD results (Section 4.2.3.1), there is no crystal structure, and at higher magnification, there are only amorphous products and unreacted particles. EDS result of point 1 in Figure 4.38d is shown in Table 4.1. The amorphous zone contains Mg and P, which can be a potential product of the reaction in Group I mixtures.

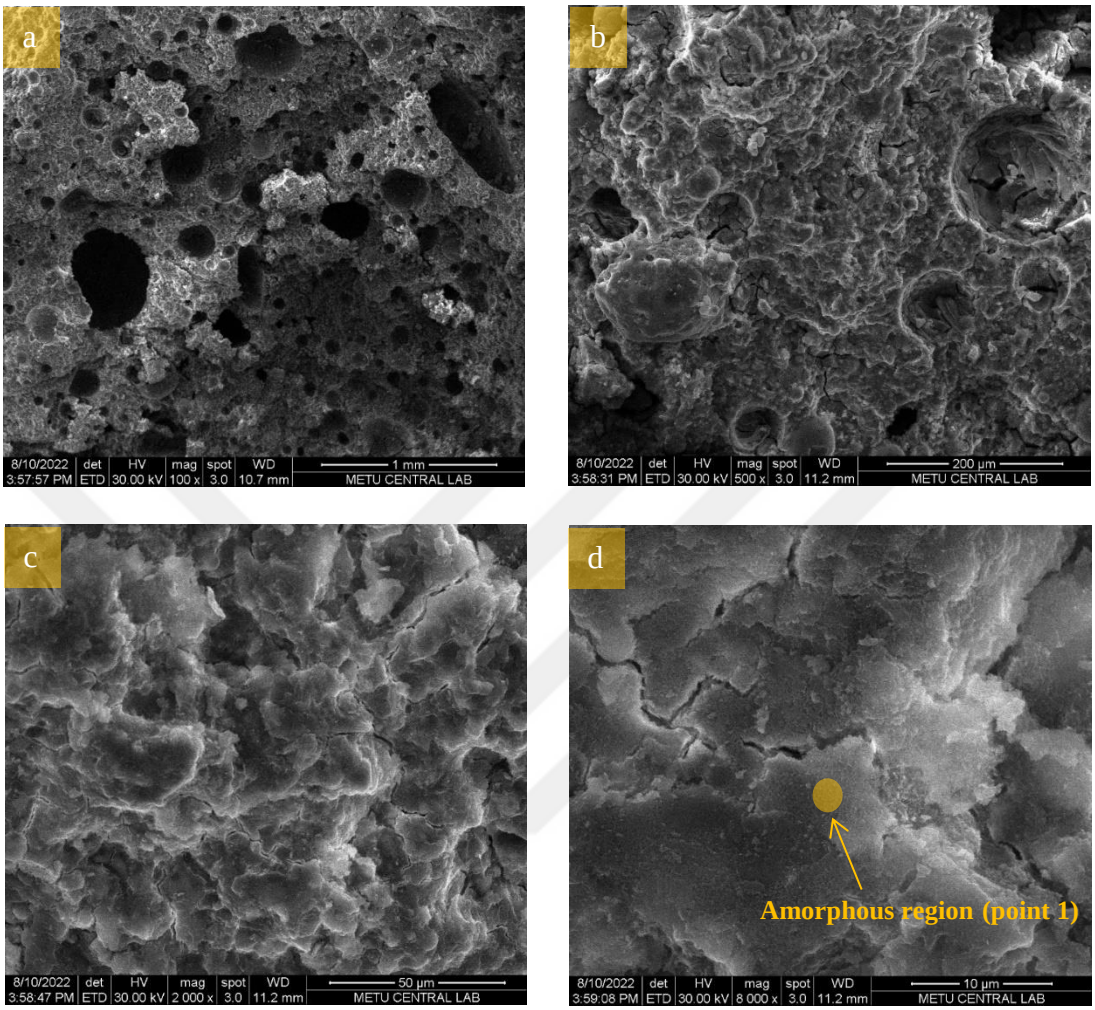


Figure 4.8 SEM images of MgFA1 (Group I)

Table 4.1 Element wt % of point 1 in Figure 4.8

Point	C	O	Na	Mg	P	K	Ca	Al	Si	Fe	S
Point 1	-	53.65	-	19.64	18.68	-	-	2.29	4.14	1.60	-

The Mg/P ratio is higher than 1, while for struvite, this ratio is 0.78, which also indicates that this product is different than struvite.

4.4.2 CxKH Mixes (Group II)

Some raw materials and amorphous structures are observed in SEM images of C1KH and C3KH (Figures 4.9d and 4.10d) consistent with XRD patterns. As shown in Figure 4.9d, besides the plate-shaped reactant crystals (point 2), gel zones can be the amorphous product. The EDS results of these points are shown in Table 4.2. At point 3, K, P, and Ca are observed which can be amorphous calcium phosphate products. However, there is no similar gel zone in the C4KH, in which the compressive strength was very low. Also, in EDS result for point 4 (Table 4.3), calcium phosphate products aren't indicated. This point can be ye'elimite, and the presence of carbon can be related to the carbonation of the ye'elimite. A low amount of Na may be coming from borax.

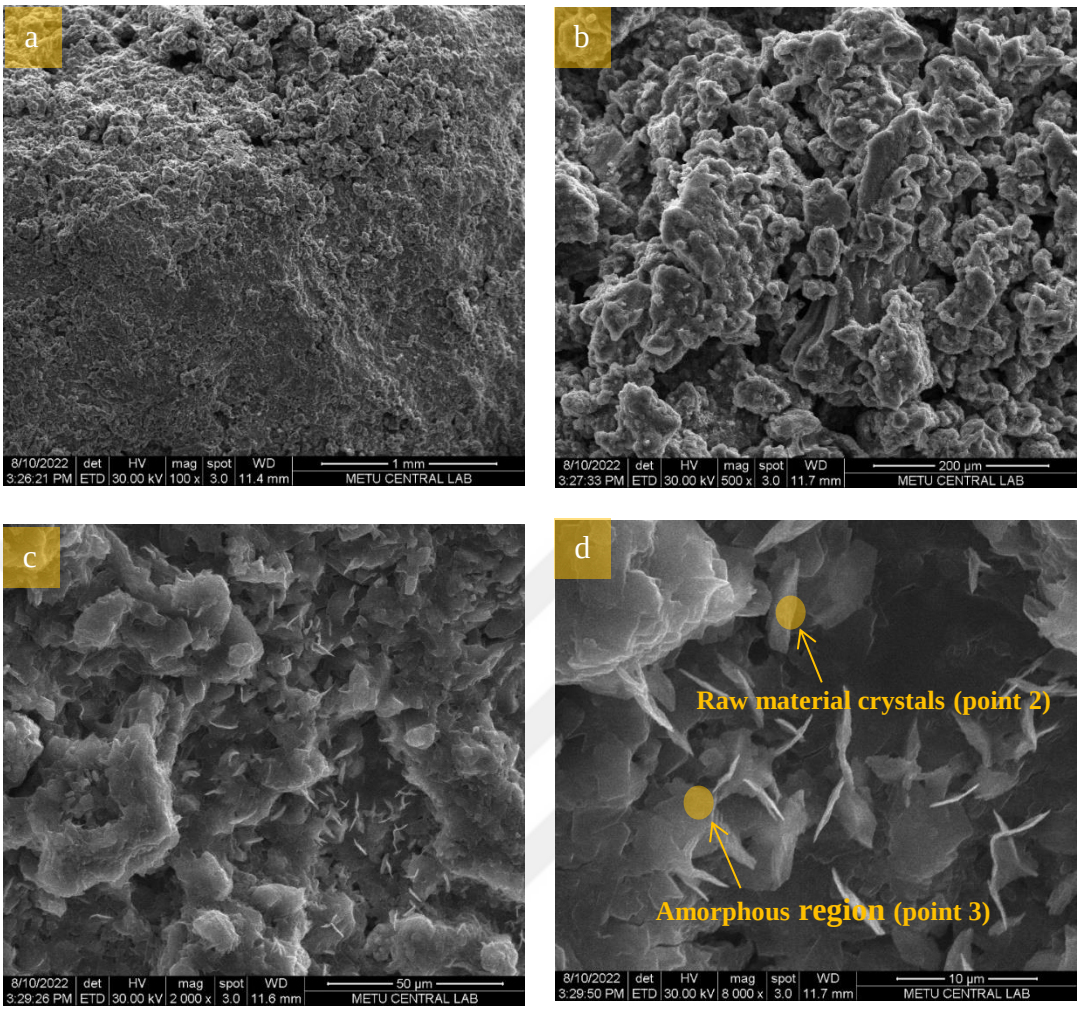


Figure 4.9 SEM images of C1KH

Table 4.2 Element wt % of points 2 and 3 in Figure 4.9

Point	C	O	Na	Mg	P	K	Ca	Al	Si	Fe	S
Point 2	15.83	36.95	1.36	-	8.47	25.06	3.50	1.53	0.69	0.48	6.13
Point 3	13.63	34.40	1.71	-	15.20	14.67	11.72	2.79	3.94	1.53	-

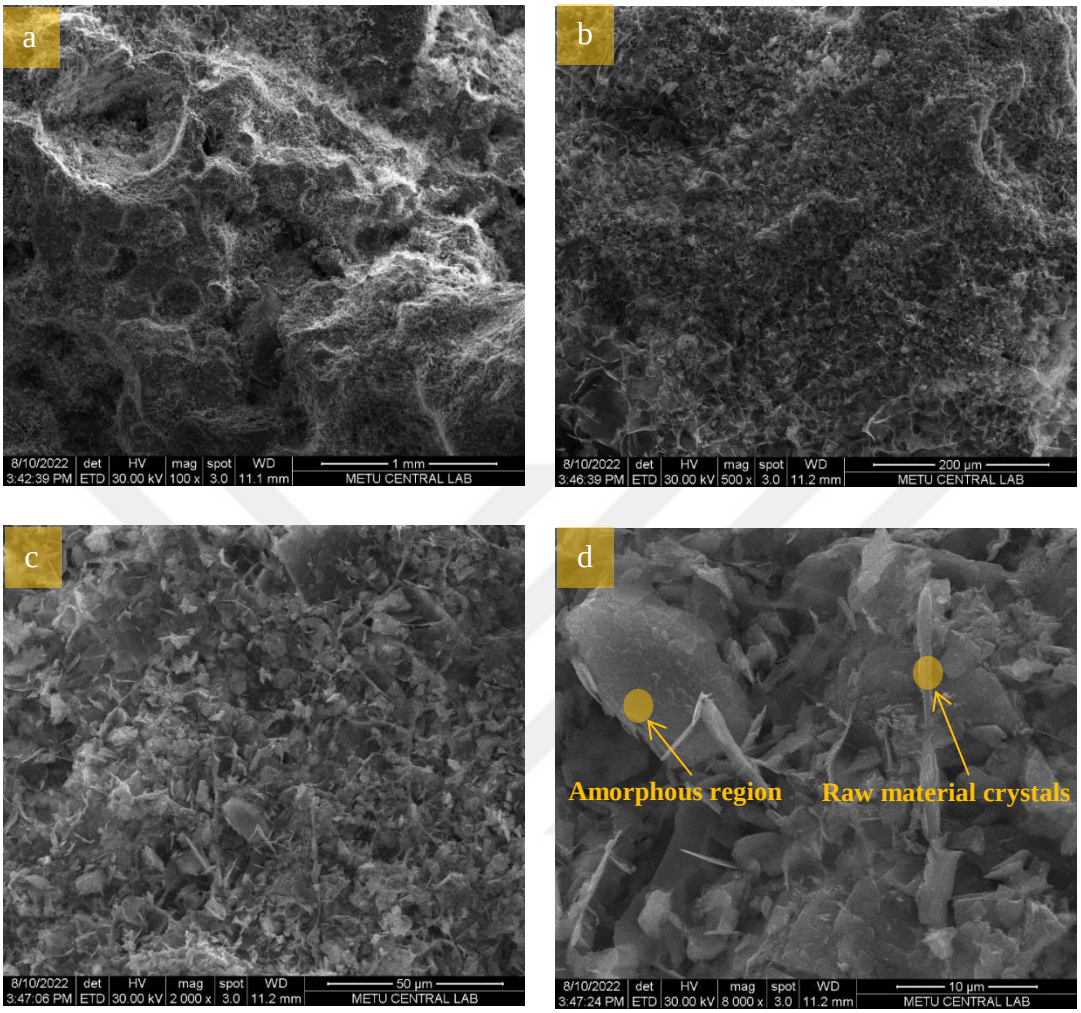


Figure 4.10 SEM images of C3KH

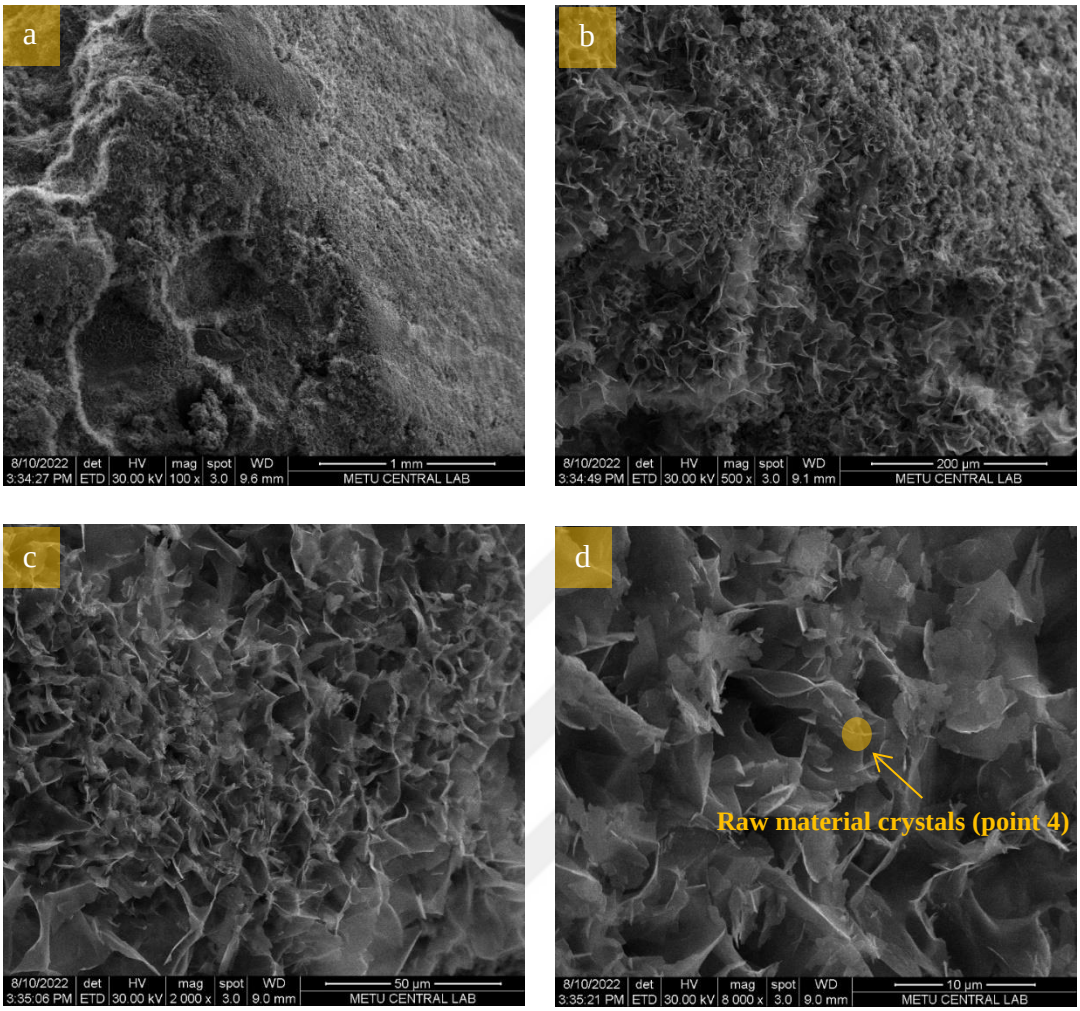


Figure 4.11 SEM images of C4KH

Table 4.3 Element wt % of point 4 in Figure 4.11

Point	C	O	Na	Mg	P	K	Ca	Al	Si	Fe	S
Point 4	11.68	33.04	1.36	-	1.14	8.27	28.57	1.79	8.42	1.44	-

4.4.3 CxFAz Mixes (Group III)

Like in MgFAz pastes, it can be seen in Figure 4.12a that a porous structure is formed in C4FA1 since the reactions happen in a very short time. At higher magnification, some spherical shapes and amorphous structures can be seen. According to the EDS results from points 5 and 6 shown in Table 4.4, it is concluded that the sphere region is the fly ash, and according to the Ca-to-P ratio at point 6, the amorphous region can be an indicator of reaction products.

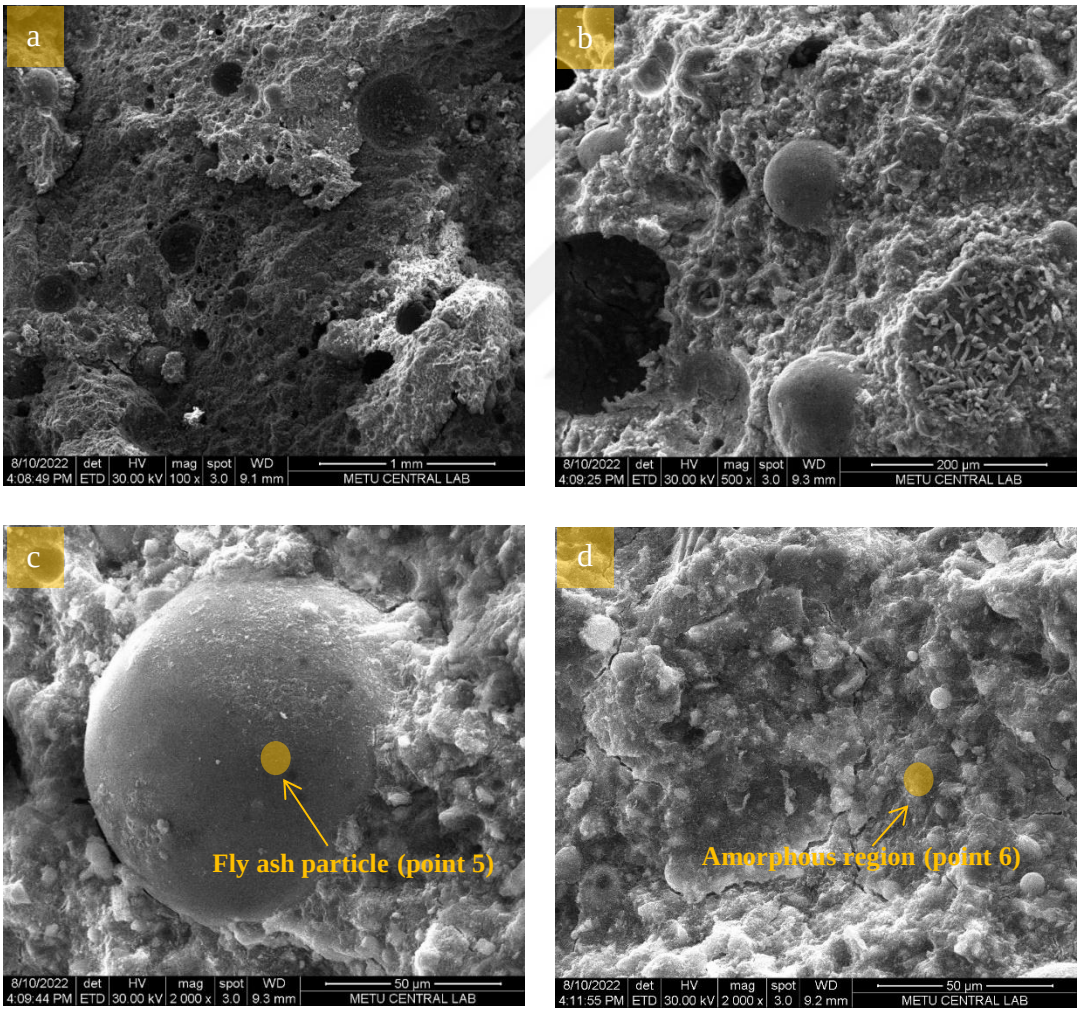


Figure 4.12 SEM images of C4FA

Table 4.4 Element wt % of points 5 and 6 in Figure 4.12

Point	C	O	Na	Mg	P	K	Ca	Al	Si	Fe	S
Point 5	-	33.76	-	-	1.27	5.96	0.74	18.05	33.26	5.06	-
Point 6	-	51.18	-	-	12.43	-	26.65	-	-	0.32	9.42

4.5 Thermogravimetric Analysis

4.5.1 Clinkers

The mass loss results of the clinkers are shown in Figure 4.13. The mass loss for all clinkers is less than 2 %, and only in C1 and C2 a mass loss is observed at 600-650 ˚C, which can be related to the calcite decomposition.

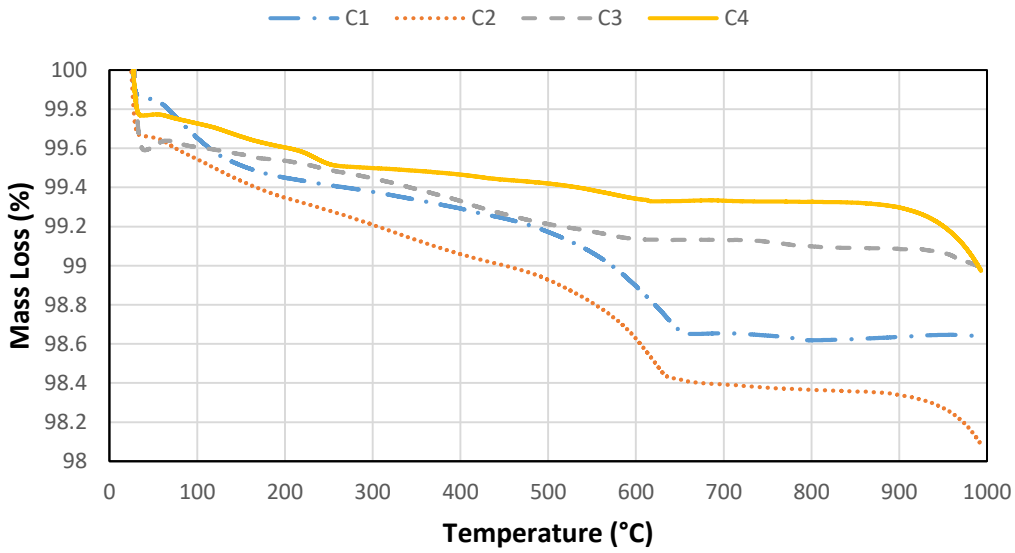


Figure 4.13 Mass loss of clinkers

4.5.2 MgFAz and CxFAz mixes (Groups I and III)

As seen in Figure 4.14, the presence of K-struvite and amorphous products can be detected at 100 and 200 °C in the reference mix. In the case of MgFA1 and C4FA1, the mass loss can be detected with a sharp slope until 200 °C due to the loss of water in the bond. In C4FA1, there isn't a mass reduction between 200 and 300 °C, but after that, up to 500 °C, there is a slight mass loss. For the mix MgFA1, there is a mass loss between 650 and 1000 °C, which can be related to the decarbonization of the products.

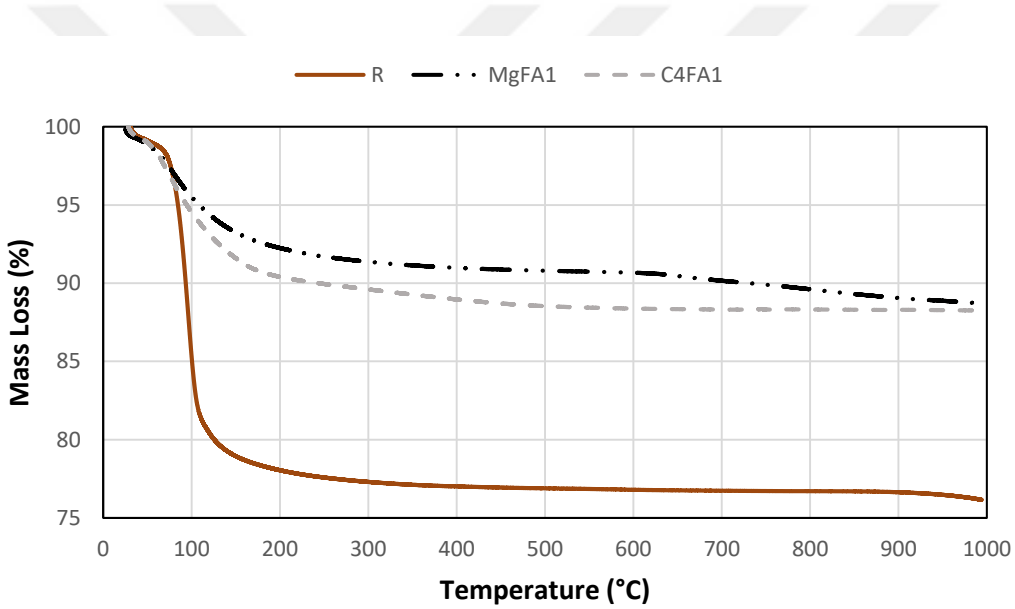


Figure 4.14 Mass loss of MgFA1, C4FA1, and reference mix

4.5.3 CxKH Mixes (Group II)

As shown in Figure 4.15, the mass loss for CxKH mixes continued up to 1000 °C, but the major part occurred before 600 °C, which means dehydration of the products. Around 200 °C, there are peaks in C1KH and C3KH, which is believed to be a loss of water bond for products. While in C4KH, this is not observed, which can explain

the low strength in this mix and the lack of strong products. Qian et al. (2020) reported one peak around 150 °C which is for K-struvite, and mass loss is constant after 200 °C, but as can be seen in Figure 4.15 a, mass loss for CxKH mixes continues until 1000 °C, that can be an indicator of amorphous structures.

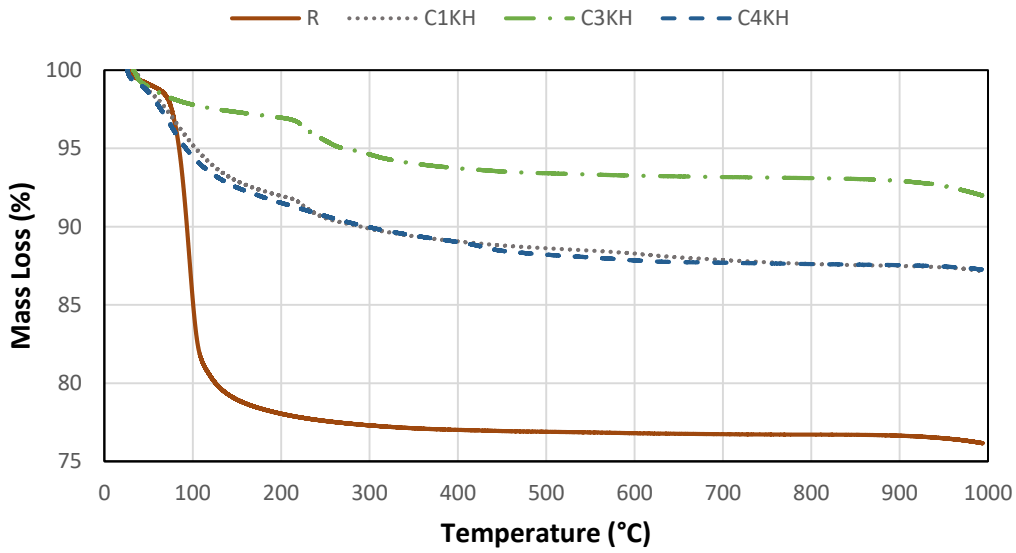


Figure 4.15 Mass loss of CxKH mixes

4.6 Resistance to Water

4.6.1 MgFAz and CxFAz Mixes (Groups I and III)

MgFA1 and C4FA1 mixes, as shown in Figure 4.16, show high resistance to water with RCS of 95.3 and 88.9 %, respectively. This can be explained by the reaction of $FAPO_4$ with MgO or C4, which produces an insoluble product at low pH. This product couldn't be detected in the XRD test, but in the SEM test, some amorphous phases were detected.

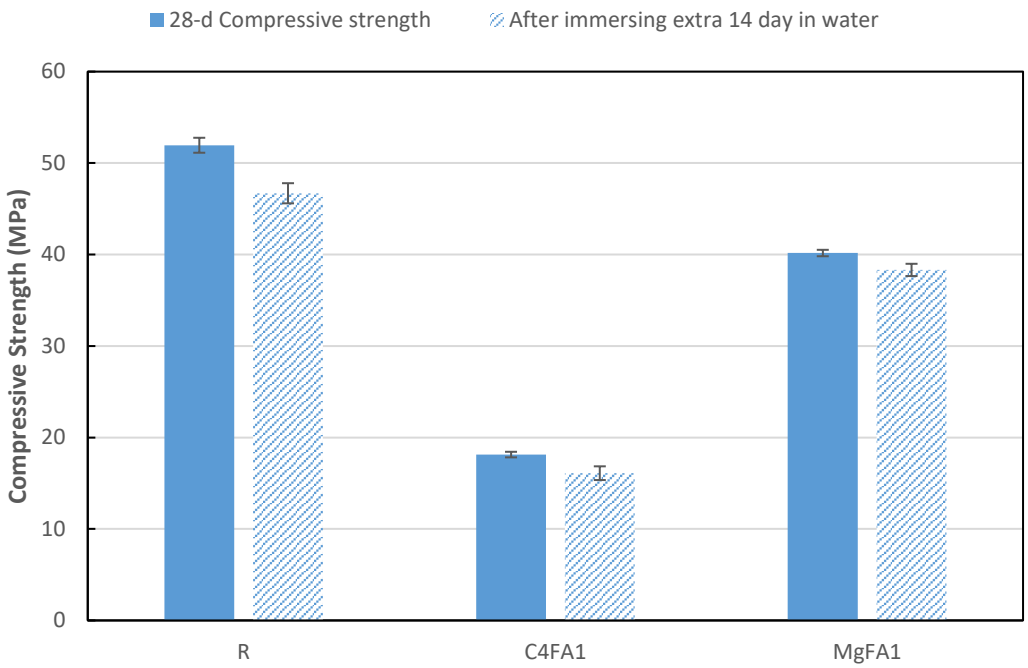


Figure 4.16 Compressive strength retention of the R, MgFA1, and C4FA1 after immersing in water

4.6.2 CxKH Mixes (Group II)

After immersing in water, CxKH loses more strength than MgFA1 and C4FA1 mixes (Figure 4.17). Since C4KH has a very low compressive strength at 28 d, this test is not done on that mixture but RCS for R, C1KH, C2KH, and C3KH, equals 84.61%, 63.00, 56.20, and 61.10 %, respectively. The use of KH_2PO_4 in these mixes can lead to amorphous products, not detectable in XRD results, which may be soluble at the lower pH caused by the dissolution of any remaining KH_2PO_4. Qian et al. (2020) reported that the compressive strength of mixtures containing sulphoaluminate clinker increases after immersing in water due to the hydration of ye'elimite, but this was not the case for CxKH mixes.

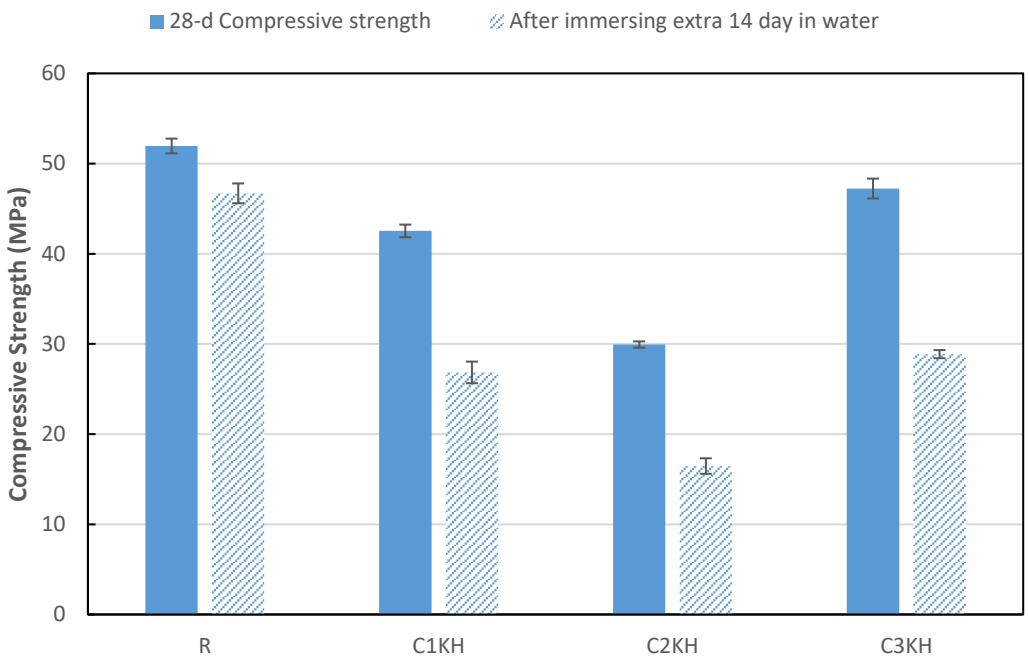


Figure 4.17 Compressive strength of the reference and CxKH mixes after immersing in water

CHAPTER 5

CONCLUSIONS AND RECOMMENDATIONS

5.1 Conclusions

In this study, three groups of phosphate cement mixtures are prepared in an effort to replace the two main acidic and basic components, KH_2PO_4 and dead-burned MgO, in magnesium phosphate cement. In Group I, KH_2PO_4 is replaced with $FAPO_4$. In Group II, MgO is replaced with $C\overline{S}A$. Finally, in Group III, both KH_2PO_4 and MgO are replaced with $FAPO_4$ and $C\overline{S}A$, respectively. The following conclusions can be drawn:

- Early compressive strength in Group I was high, but the setting time was less than the reference mix. This can be related to the low initial pH in the acidic solution obtained using $FAPO_4$.
- Compressive strength development in Groups I and III didn't continue remarkably after 7 d. However, in Group II, the compressive strength increased until 28 d. In C3KH, 28 d compressive strength was close to those of the reference and Group I.
- C4FA (Group III) had low compressive strength compared to Groups I and II. However, it didn't show a reduction in compressive strength between 7 d and 28 d, unlike Group I.
- Setting time in Groups I and III was shorter than 5 minutes. However, Group III mixtures had 4-7 h setting time. In Group II, since KH_2PO_4 and $C\overline{S}A$ were used together, the reactions occurred slower. Also the lower early strength of Group II in comparison to two other groups can be related to this.
- Products of reactions in all mixtures except the reference were amorphous according to XRD, TGA, and SEM analysis. In the SEM and EDS analyses of Group II and III, gel-like zones were composed mostly of Ca and P

indicates the formation of calcium phosphates. In Group I, gel-like particles were composed of Mg and P. These can be indicators of amorphous products.

- Among the mortars prepared with four selected calcium sulphoaluminate clinkers, those made with C4 didn't gain strength higher than 6 MPa and 17 MPa in Group II and III, respectively. This can be because of the minerals like gehlenite in this cement, which didn't lead to strong minerals in the reaction with phosphates.
- Water resistance in this study was evaluated using residual compressive strength (RCS) after exposure to water. Groups I and III showed high resistance to water with RCS of 95.3 and 88.9 %, which is higher than that of the reference mix, 84.6 %. On the other hand, Group II had the lowest RCS among the three groups of mixes, approximately 60 %.
- The higher early compressive strength and short setting time in Group I makes it a potential repairing material. However, Group II with a long setting time can be appropriate for construction applications.
- Besides the all properties obtained in three mixture groups, using C$\overline{S}$A is environmentally friendly and less expensive in comparison to MgO.

5.2 Recommendations for Future Studies

The following can be recommended for future studies:

- Since the initial pH in the acidic solution has a significant role in the setting time of MPC, diluted phosphoric acid can be helpful to increase the setting time.
- Mixtures with combined MgO and calcium sulphoaluminate clinker can imitate the drawbacks of each mixtures groups. For example, low compressive strength in C4FA, or low early compressive strength in CxKH samples can be improved by partially replacing clinkers with MgO. Also,

replacement of MgO with C4 in Group I can reduce the strength loss between 7 d and 28 d.

- Different $FAPO_4$ can be produced with different fly ashes to compare their effects.
- The partial replacement of clinker with MgO can be done at the calcination stage. Different proportions of raw magnesium oxide can be mixed with raw materials for CSA cement to be calcined at 1300 °C.

REFERENCES

ASTM C618 (2022). Standard Specification for Coal Fly Ash and Raw or Calcined Natural Pozzolan for Use in Concrete. ASTM international,West Conshohocken, PA.

ASTM C33/C33M (2018). Standard Specification for Concrete Aggregates. ASTM International, West Conshohocken, PA.

ASTM C191 (2021). Standard Test Methods for Time of Setting of Hydraulic Cement by Vicat Needle. ASTM International, West Conshohocken, PA.

ASTM D7348 (2021). Standard Test Methods for Loss on Ignition (LOI) of Solid Combustion Residues. ASTM International, West Conshohocken, PA.

Bilginer, B. A., Erdoğan, S. T. (2021). Effect of mixture proportioning on the strength and mineralogy of magnesium phosphate cements. *Construction and Building Materials, 277*. https://doi.org/10.1016/j.conbuildmat.2021.122264

Bentz, D. P. (2010). Blending different fineness cements to engineer the properties of cement-based materials. *Magazine of Concrete Research, 62*(5), 327–338. https://doi.org/10.1680/macr.2008.62.5.327

Bilginer, B. A., Erdoğan, S. T. (2021). Effect of mixture proportioning on the strength and mineralogy of magnesium phosphate cements. *Construction and Building Materials, 277*. https://doi.org/10.1016/j.conbuildmat.2021.122264

Canbek, O. & Erdoğan, S. T. (2020). Influence of production parameters on calcium sulfoaluminate cements. *Construction and Building Materials, 239*. https://doi.org/10.1016/j.conbuildmat.2019.117866

Feng, H., Nie, S., Guo, A., Lv, L. & Yu, J. (2022). Evaluation on the performance of magnesium phosphate cement-based engineered cementitious composites (MPC-ECC) with blended fly ash/silica fume. *Construction and Building Materials, 341*. https://doi.org/10.1016/j.conbuildmat.2022.127861

Hall, D. A., Stevens, R. & El-Jazairi, B. (2001). The effect of retarders on the microstructure and mechanical properties of magnesia-phosphate cement mortar. *Cement and Concrete Research*, *31*(3), 455–465. https://doi.org/10.1016/S0008-8846(00)00501-9

Hanein, T., Galvez-Martos, J. L. & Bannerman, M. N. (2018). Carbon footprint of calcium sulfoaluminate clinker production. *Journal of Cleaner Production, 172*, 2278–2287. https://doi.org/10.1016/j.jclepro.2017.11.183

Jabri, M., Mejdoubi, E., El Gadi, M. & Hammouti, B. (2012). Optimisation of hardness and setting time of dental zinc phosphate cement using a design of experiments. *Arabian Journal of Chemistry, 5*(3), 347–351. https://doi.org/10.1016/j.arabjc.2010.09.004

Jia, L., Zhao, F., Guo, J. & Yao, K. (2019). Magnesium Phosphate Cement Mixed with Ferroaluminate Cement. *Materials*, 15. https://doi.org/10.3390/ma12162561

Le Rouzic, M., Chaussadent, T., Platret, G. & Stefan, L. (2017). Mechanisms of k-struvite formation in magnesium phosphate cements. *Cement and Concrete Research*, *91*, 117–122. https://doi.org/10.1016/j.cemconres.2016.11.008

Li, J., Xu, G., Chen, Y. & Liu, G. (2014) multiple scaling investigation of magnesium phosphate cement modified by emulsified asphalt for rapid repair of asphalt mixture pavement. *Construction and Building Materials*, *69*, 346–350. https://doi.org/10.1016/j.conbuildmat.2014.07.079

Li, K., Shen, Q. Y., Xie, Y. T. & Zheng, X. Bin. (2014). Preparation and characterization of calcium-magnesium phosphate cements. *Advanced Materials Research*, *1058*, 83–86. https://doi.org/10.4028/www.scientific.net/AMR.1058.83

Li, Y. & Chen, B. (2013). Factors that affect the properties of magnesium phosphate cement. *Construction and Building Materials*, *47*, 977–983. https://doi.org/10.1016/j.conbuildmat.2013.05.103

Li, Y., Shi, T. & Li, J. (2016). Effects of fly ash and quartz sand on water-resistance and salt-resistance of magnesium phosphate cement. *Construction and Building Materials*, *105*, 384–390. https://doi.org/10.1016/j.conbuildmat.2015.12.154

Li, Y., Sun, J. & Chen, B. (2014). Experimental study of magnesia and M/P ratio influencing properties of magnesium phosphate cement. *Construction and Building Materials*, *65*, 177–183. https://doi.org/10.1016/j.conbuildmat.2014.04.136

Liu, N. & Chen, B. (2016). Experimental research on magnesium phosphate cements containing alumina. *Construction and Building Materials*, *121*, 354–360. https://doi.org/10.1016/j.conbuildmat.2016.06.010

Liu, Y., Qin, Z. & Chen, B. (2020). Influence of low-grade bauxite on the properties of magnesium phosphate cement. *Construction and Building Materials*, *242*. https://doi.org/10.1016/j.conbuildmat.2020.118052

Luong, V. T., Amal, R., Scott, J. A., Ehrenberger, S. & Tran, T. (2018). a comparison of carbon footprints of magnesium oxide and magnesium hydroxide produced from conventional processes. *Journal of Cleaner Production*, *202*, 1035–1044. https://doi.org/10.1016/j.jclepro.2018.08.225

Mahyar, M. & Erdoğan, S. T. (2015). Phosphate-activated high-calcium fly ash acid-base cements. *Cement and Concrete Composites*, *63*, 96–103. https://doi.org/10.1016/j.cemconcomp.2015.09.002

Mo, L. (2018). Carbon dioxide sequestration on steel slag. In *Carbon Dioxide Sequestration in Cementitious Construction Materials* (pp. 175–197). Elsevier. https://doi.org/10.1016/B978-0-08-102444-7.00008-3

Qiao F., Chau C.K.. Li Z. (2010 a). Setting and strength development of magnesium phosphate cement paste. Advances in Cement Research, 21, 175 - 180. https://doi.org/10.1680/adcr.9.00003

Qiao, F., Chau, C. K. & Li, Z. (2010 b). Property evaluation of magnesium phosphate cement mortar as patch repair material. *Construction and Building Materials*, *24*(5), 695–700. https://doi.org/10.1016/j.conbuildmat.2009.10.039

Ruan, W., Ma, Y., Liao, J., Ma, T., Zhu, Y. & Zhou, A. (2022). Effects of steel slag on the microstructure and mechanical properties of magnesium phosphate cement. *Journal of Building Engineering*, *49* https://doi.org/10.1016/j.jobe.2022.104120

Soudée, E. & Péra, J. (2000). mechanism of setting reaction in magnesia-phosphate cements. *Cement and Concrete Research*, 30. https://doi.org/10.1016/S0008-8846(99)00254-9

Wagh, A. S. (2016). Introduction to Chemically Bonded Ceramics. In *Chemically Bonded Phosphate Ceramics* (pp. 1–16). Elsevier https://doi.org/10.1016/b978-0-08-100380-0.00001-4.

Wang, A. J., Zhang, J., Li, J. M., Ma, A. B. & Liu, L. T. (2013). Effect of liquid-to-solid ratios on the properties of magnesium phosphate chemically bonded ceramics. *Materials Science and Engineering C*, *33*(5). https://doi.org/10.1016/j.msec.2013.02.014

Wang, X., Hu, X., Yang, J., Chong, L. & Shi, C. (2022). Research progress on interfacial bonding between magnesium phosphate cement and steel: A review. In *Construction and Building Materials*, 342. Elsevier Ltd. https://doi.org/10.1016/j.conbuildmat.2022.127925

Watanabe, M., Tanaka, M., Sakurai, M. & Maeda, M. (2006). Development of calcium phosphate cement. *Journal of the European Ceramic Society*, *26*(4–5), 549–552. https://doi.org/10.1016/j.jeurceramsoc.2005.07.003

Wilson, A. D. and Nicholson, J. W. (2005). Acid-base cements: Their biomedical and industrial applications. England, Cambridge, Cambridge University Press.

Xu, B., Lothenbach, B. & Winnefeld, F. (2020). Influence of wollastonite on hydration and properties of magnesium potassium phosphate cements. *Cement and Concrete Research, 131*. https://doi.org/10.1016/j.cemconres.2020.106012

Yang, J. & Qian, C. (2010). Effect of borax on hydration and hardening properties of magnesium and potassium phosphate cement pastes. *Journal of Wuhan University of Technology-Mater. Sci. Ed.*, *25*(4), 613–618. https://doi.org/10.1007/s11595-010-0055-6

Yang, Q., Zhu, B. & Wu, X. (2000). Characteristics and durability test of magnesium phosphate cement-based material for rapid repair of concrete. *Materials and Structures*, *33*(4), 229–234. https://doi.org/10.1007/bf02479332

Yu, J., Qian, J., Wang, F., Li, Z. & Jia, X. (2020). Preparation and properties of a magnesium phosphate cement with dolomite. *Cement and Concrete Research*, *138*, 106235. https://doi.org/10.1016/j.cemconres.2020.106235

Zhang, Q., Cao, X., Ma, R., Sun, S., Fang, L., Lin, J. & Luo, J. (2021). Solid waste-based magnesium phosphate cements: Preparation, performance and solidification/stabilization mechanism. *Construction and Building Materials* (Vol. 297). Elsevier Ltd. https://doi.org/10.1016/j.conbuildmat.2021.123761

APPENDICES

APPENDIX A

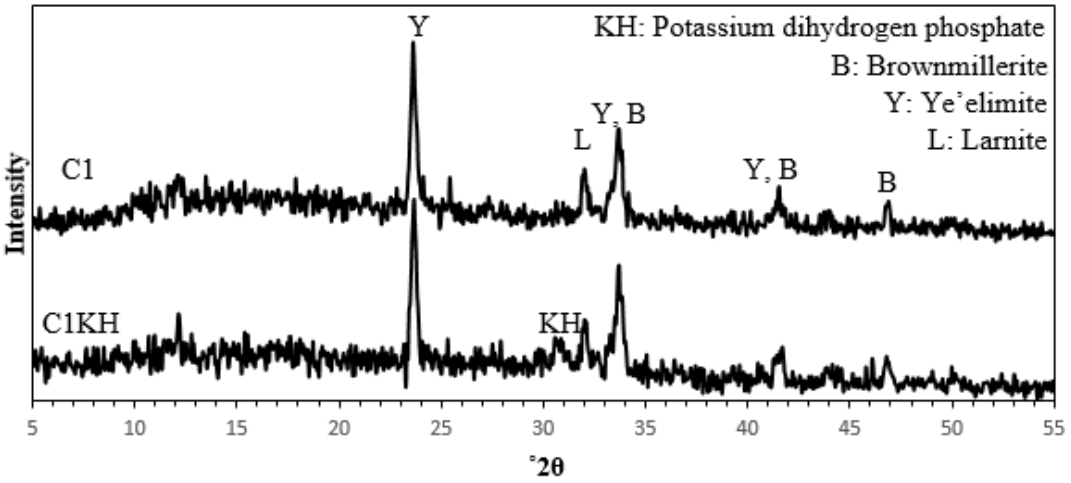


Figure A.1 XRD patterns of C1 and C1KH

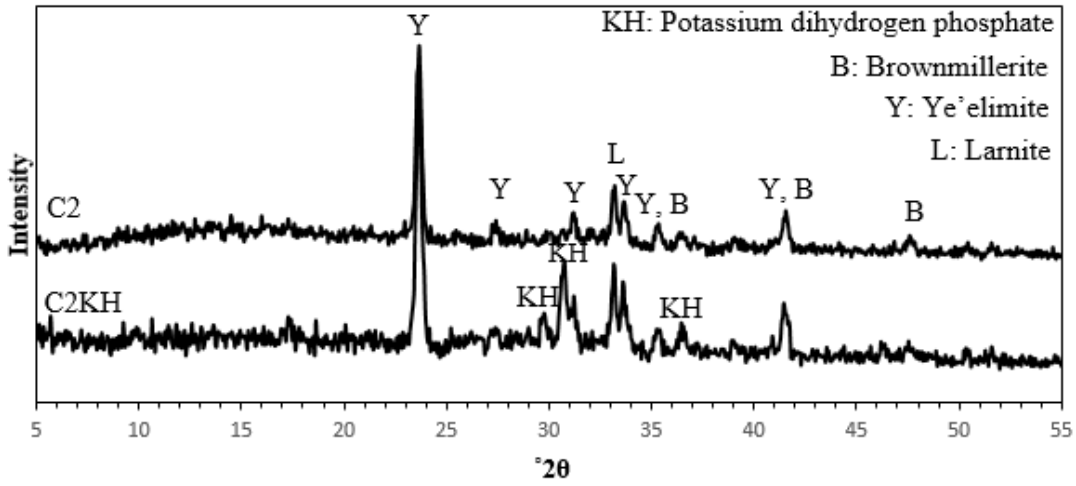


Figure A.2 XRD patterns of C2 and C2KH

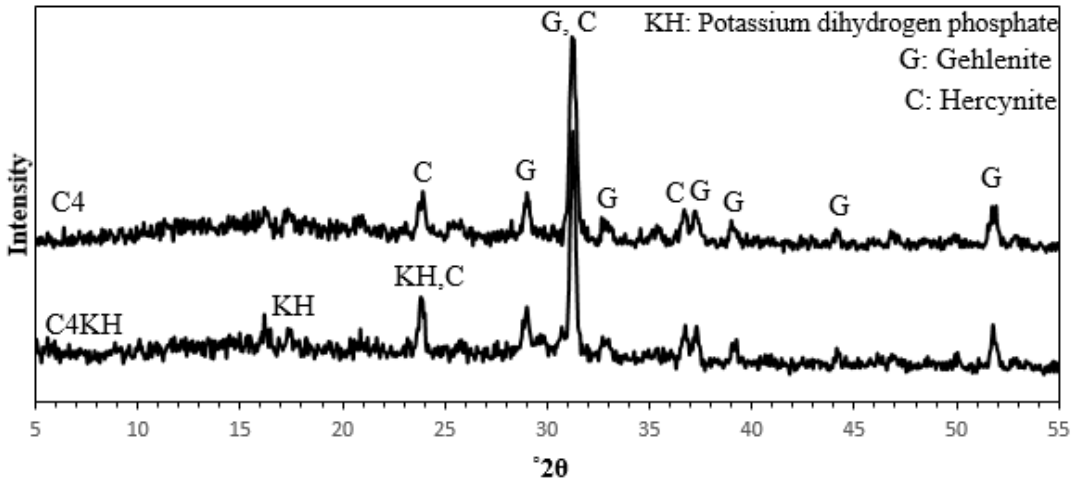


Figure A.3 XRD patterns of C4 and C4KH